Università di Roma "La Sapienza"
Dipartimento di Fisica

Dottorato di ricerca in Fisica, X ciclo

Structure of metastable states in spin glasses by means of the three-replica potential

Ph.D. thesis of Irene Giardina

Supervisor: Professor Giorgio Parisi

The original work exposed in this thesis has been realized in collaboration with Giorgio Parisi and Andrea Cavagna, and inherited the contribution of many people who stimulated us with precious suggestions and discussions. I would like to thank them all and especially Alain Barrat, Jean-Philippe Bouchaud, Premi Chandra, Leticia Cugliandolo, Silvio Franz, Jorge Kurchan, Marc Mézard, Rémi Monasson, Heiko Rieger, Felix Ritort, Juan Jesús Ruiz-Lorenzo, David Ruelle, David Sherrington and Miguel Angel Virasoro.

I particularly thank Giorgio for his intellectual and human accompanying in these years and Andrea, who shared with me all this.

Contents

Introduction

The mean field theory of spin-glasses has been longly developed in these last years. What has clearly emerged is that the low temperature phase of mean-field models is characterized by the presence of a huge number of pure states. The general guess is that such complicated free-energy landscapes still survive in finite dimension and are the actual responsible of the physics of real complex systems.

It is possible to distinguish two classes of mean-field models, according to the order of the freezing transition:

- There are models, like the famous Sherrington Kirkpatrick model (SK) [1], which display a second order continuous statical transition. In these models the equilibrium properties of the system in the low temperature phase are determined only by the states with the lowest energy density, that is by the stable states, while states with higher energy density, the so called metastable states, do not play any role [2]. The stable states are also the ones relevant for the dynamics and the asymptotic limits of the dynamical extensive quantities coincide with the corrispondent equilibrium values [3,4].
- The second class is constitued by models which present a discontinuous first order transition, like the p-spin models (Ising, soft and spherical), the Potts glasses and others [5,6,7,8]. For these models the metastable states turn out to be fundamental in determining both the statical and the dynamical behaviour of the system. From a statical point of view, there is a temperature range in which the partition function is dominated by an appropriate class of metastable states. Moreover, the dynamical quantities tend asymptotically to values corresponding to metastable states which are not the equilibrium ones [9,10].

At present it is commonly belived that, while the first class of these models is quite appropriate to describe real spin-glasses, the second one is closer to describe the physics of structural glasses and therefore in these last years has become subject of a deep theorical investigation. The reason is that the models of the second class present some dynamical features which seem to be compatible with the phenomenology observed in glasses. In particular, it is known that these models have a dynamical transition at a temperature T_d which is *greater* than the temperature T_s at which the static transition takes place [11,12], while for models of the first class the two temperutures coincide. This means that at T_d the transition is purely dynamical, the relaxation time diverges but all the thermodynamic quantities do not show any singularity. What observed in real glasses is similar, in the sense that the glass transition is actually a purely dynamical effect. The glassy temperature T_{glass} is defined as the temperature at which the relaxation time reaches a value greater than the usual observation times of the experiments. The question if there is a true transition at a lower temperature is still controversial, anyway it would happen at a temperature $T_0 < T_{glass}$ [13].

If one considers corrections to mean field theory the physics of spin-glass models of the second class presumably becomes still more similar to the phenomenological scenario of real glasses. The models of the second class are characterized by the presence of a big number of metastable states which, in the mean field approximation, are separated by infinite barriers and thus have infinite life-time. This is also the reason for which some of them are able to trap the system in the asymptotic dynamics. In the correspondent short range models the situation is different: there cannot be metastable states divided by infinite barriers, since enucleation processes would bring in a finite time from a metastable state to the stable one [7,11,14]. Yet it is reasonable that the structure of the states present in the mean field models would in some sense survive: one can imagine a picture in which there still are metastable states, but separated by finite barriers. In this context there would not be a dynamical transition at T_d, but the system would remain in a metastable state for a certain finite time and then jump away [15]. T_d would then represent a cross-over temperature below which activated processes become important, while the real transition would happen at the lower temperature T_s.

The case of the p-spin spherical model is still more interesting. Indeed for $T > T_d$ the dynamical equations for this model are surprisingly analogous to the mode-coupling equations for super-cooled liquids [13,9,16]. Moreover for $T < T_d$ the dynamics has been analitically solved revealing a strong off-equilibrium ageing behaviour qualitatively similar to the one really observed in the experiments on glasses.

For these reasons this model seems to be a good mean-field candidate for real glasses and a deep understanding of its features can be an important step towards the comprehension of the physics of glasses.

We have already stressed that a peculiaruty of this model is the presence of a huge number of metastable states which are relevant both in the statics and the dynamics of the system. Therefore it is surely an interesting problem to investigate the geometrical organization of these states, that is how they are disposed in the phase-space.

The description of the structure of the states often is the key point in understanding a model. The Sherrington Kirkpatrick model is maybe the best example: for it the ultrametric structure of the equilibrium stable states represents the unifyng frame in which all the properties of the model are fully explained [17,18,19] [2,20]. It would be appealing to find out something equivalent also for the p-spin model, in which *all* the states, both stable and metastable, are relevant.

Moreover there is another important reason to investigate the structure of the states. We have seen that the strongest connection with glasses takes place whenever corrections to mean field are considered. The times to escape from state to state are in this case exponentially high in N, but finite, and thus the dynamics is dominated at ultra large times by the crossing of the free energy barriers between different states. This can also be, as we previously said, the mechanism of the eventual smearing out of the dynamical transition in the short range model. It is evident that this kind of dynamics is highly dependent on the local structure of the phase-space and thus some useful information can be gathered analyzing the mutual disposition of the states and computing the barriers separating them.

In the case of the p-spin spherical model the standard statistical approaches have not been able to clarify what is the structure of the states. Apparently they seem to suggest that this structure is trivial, but actually they are not enough sophisticated to deal with this question. Thus it has been necessary to invent non standard methods first of all to verify that a non trivial structure of the states indeed exists, and then to obtain detailed information on it.

In this PhD thesis we will expone one of these methods and the results that have been obtained with it [21,22,23,24]. This method is mainly based on the statical analysis of constrained systems and lies in the general context of the *Real Replica method.* The fundamental idea is very simple. One studies a system which is subjected to satisfy some external constraints. Because of the constraints the system is forced to thermalize in a restricted region of the phase-space. The hope is that, by varying the constraints, it is possible to induce the system to thermalize into a metastable state, thus revealing its presence.

The discussion is organized in the following way. In Chapter I we will introduce the model and briefly summarize the principal results that have been obtained on it with the usual statical methods. We will show that these methods do not provide enough information on the structure of the states and explain why. In Chapter II we will introduce the method that we have applied to face the problem and in particular the basic quantity of our analysis, the potential function. We will show how this method works in the simpler case of the two-replica potential, and explain why it is yet not enough refined to pursue the aim. In Chapter III we will define and compute the three-replica potential and discuss all the results that are obtained with it on the structure of the states. In chapter IV we will compare the results of the constrained systems method with another method that has been parallely developed in the different context of the *TAP approach* [25,26,27,28]. In Chapter V we will return back to the Real Replica method to obtain an estimate of the barriers separating different metastable states. Finally, in the conclusions we will comment the whole analysis and outline the frame of a possible forecoming research on this topic.

Chapter I: A general overview

1. The model

The p-spin spherical model [6,29,7,5] is defined by the Hamiltonian

$$
\begin{aligned}
H(\sigma) &= \sum_{i_1<i_2<\ldots<i_p} J_{i_1\ldots i_p}\sigma_{i_1}\ldots\sigma_{i_p} \\
\frac{1}{N}\sum_i \sigma_i^2 &= 1
\end{aligned}
\tag{1.1}
$$

where the σ_i are real variables satisfying the spherical constraint and the couplings $J_{i_1\ldots i_p}$ are independent Gaussian variables with variance

$$
\overline{J^2_{i_1\ldots i_p}} = \frac{p!}{2N^{p-1}} \ . \tag{1.2}
$$

Due to the spherical constraint the phase space of this model is an N-dimensional sphere with radius $\sqrt{N}$ and the configurations are vectors lying on it. The overlap between two configurations measures how much these configurations are similar and is defined in the usual way:

$$
q_{\sigma\sigma'} = \frac{1}{N}\sum_i \sigma_i {\sigma'}_i \ . \tag{1.3}
$$

One can give a simple geometrical interpretation of the overlap (1.3): it represents the scalar product of the vectors σ and σ' and is proportional to the cosine of the angle between them. In this context two coinciding configurations have a vanishing angle and mutual overlap equal to 1, while two very far configurations are mutually orthogonal on the sphere and have overlap equal to zero.

This model is characterized in the low temperature phase by the presence of many pure states, whose structure in the phase space is the principal subject of this thesis. In this context it is crucial to extend the previous definition of overlap and adapt it to measure the similarity between two pure states. In this way a notion of 'distance' between states is introduced and with respect to it a quantitative analysis of the mutual disposition of the states becomes meaningful. Given two pure states a and b their mutual overlap q_{ab} is defined as

$$
q_{ab} = \frac{1}{N}\sum_i <\sigma_i>_a <\sigma_i>_b = \frac{1}{N}\sum_i m_i^a m_i^b \tag{1.4}
$$

where $< ... >_a$ indicates the average with the measure identifying the pure state a, and m^a is the magnetization evaluated with it. With the same procedure the self-overlap of an individual pure state a is defined considering twice the same state in (1.4)

$$q_{aa} = \frac{1}{N} \sum_i (< \sigma_i >_a)^2 = \frac{1}{N} \sum_i (m_i^a)^2 \tag{1.5}$$

In this way q_{ab} represents the typical overlap between a configuration of the state a and one of the state b, while q_{aa} represents the typical overlap between two configurations belonging to the same state a. The more a and b are similar, the more their mutual overlap q_{ab} will be high. The limiting case in which the mutual overlap q_{ab} is identical to the self-overlaps q_{aa} and q_{bb} of the individual states means that a and b actually coincides. On the other hand when the overlap between two states is zero, they are completely different and their supports on the phase space are approximately orthogonal.

The static of this model has been studied basically with two different approaches: the Replica approach and the TAP approach. We will now examine in more details what these two approaches show (see also [30]).

2. The Replica approach

In the Replica approach one directly computes the free-energy density F of the system [2]. This calculation is absolutely not trivial since it involves the average over the disorder of the logarithm of the partition function. To handle this problem one resorts to use the replica trick.

The free energy density F is expressed in terms of a set $\{\sigma_a\}$ of n identical replicas of the system, exploiting the following relation:

$$\begin{aligned} -\beta F &= \frac{1}{N} \lim_{n\to 0} \frac{\log \overline{Z^n}}{n} \; . \\ &= \frac{1}{N} \lim_{n\to 0} \frac{1}{n} \log \int \mathcal{D}\sigma_a \exp\left[-\beta \sum_{a=1}^{n} \mathcal{H}(\sigma_a) \right] \end{aligned} \tag{2.1}$$

The general strategy is then to compute (2.1) with n finite, and then perform the analytic continuation for $n \to 0$.

For the p-spin spherical model this calculation has been performed in [5]. After averaging over the interactions, uncoupling the sites, and partially using the saddle point equations, expression (2.1) becomes:

$$-\beta F = \operatorname*{Ext}_Q \left\{ \lim_{n\to 0} \frac{1}{2n} \left(\beta^2 \sum_{a,b} f(Q_{ab}) + \log \det Q \right) \right\} \tag{2.2}$$

where the function f is defined by

$$N \frac{1}{2} f(q_{\sigma,\sigma'}) = \overline{H(\sigma) H(\sigma')} = N \frac{1}{2} q_{\sigma\sigma'}^p \; . \tag{2.3}$$

and

$$Q_{ab} = q_{\sigma_a \sigma_b} \quad a = 1, \ldots, n \quad b = 1, \ldots, n \tag{2.4}$$

is the overlap matrix between different replicas, which is by definition symmetric and has the diagonal fixed to one by the spherical constraint.

To perform the remaining saddle point in (2.2) one has to choose an ansatz for the overlap matrix Q. If one works in the context of the Parisi ansatz [2] it turns out that there exists a temperature T_s such that

- For $T > T_s$ the correct solution is the RS (Replica Symmetric) one

$$Q_{ab} = q \; ; \quad a \neq b \; . \tag{2.5}$$

  and the saddle point equation gives as solution $q = 0$. The values of the thermodynamic quantities are equal to the paramagnetic ones, in particular

$$F_{RS} = F_{para} = -\frac{\beta}{4} \tag{2.6}$$

- For $T < T_s$ the correct solution is a one-step RSB (Replica Symmetry Broken) solution: Q is divided in sub-matrices of size x and a different variational parameter is chosen for the diagonal blocks and the off-diagonal ones, that is

$$Q_{ab} = (1 - q_1)\, \delta_{ab} + (q_1 - q_0)\, \epsilon_{ab} + q_0 \tag{2.7}$$

  where ϵ_{ab} is equal to one in the diagonal blocks and zero elsewhere. The correspondent expression for the free energy density is

$$-2\beta F = \operatorname*{Ext}_{q_0, q_1, x} \left\{ \beta^2 + \beta^2 (x-1) f(q_1) - \beta^2 x f(q_0) + \log(1 - q_1) + \frac{1}{x_r} \log\left(1 + x \frac{q_1 - q_0}{1 - q_1}\right) \right\} \; . \tag{2.8}$$

  The saddle point equations gives $q_0 = 0$ in absence of external magnetic field, as in our case, therefore the non trivial variational parameters are $0 < q_1 < 1$ and $x < 1$.

At T_S the transition from the RSB solution to the RS one is discontinuous in the order parameter, that is $q_1(T_s) \neq 0$, but the free energy remains continuous since $x(T_s) = 1$.

For $T > T_s$ the RSB solution is still thermodynamically stable, even if with $x > 1$, but one has to choose the RS one because it corresponds to a lower free energy density. However this fact is an important indication of the presence of metastable states above T_S. Usually an RS solution corresponds to a single paramagnetic ergodic component, while an RSB solution corresponds to a phase in which a lot of pure states are present. Indeed this picture reveals to be true for spin-glass models of the first class, and for them the static transition actually consists in an ergodicity breaking of the phase-space. On the other hand this is not what happens for models of the second class, and in particular for the p-spin spherical model. The presence of metastable states suggests that also above the static transition temperature there are more than one ergodic component. Indeed we will show in the next section that the metastable states above T_s are very numerous and the interpretation of the RS solution and of the statical transition is in this case different.

In the replica formalism it is possible to define and compute a quantity that gives information on the distribution of the pure states in the low temperature phase [2]. This quantity is the averaged overlap distribution $P(q)$ of the states and is defined in the following way

$$P(q) = \overline{\sum_{a,b} w_a w_b \ \delta(q - q_{ab})} \tag{2.9}$$

that is, $P(q)$ is the probability that, picked up two pure states, their mutual overlap is equal to q. We note that in the distribution $P(q)$ two different contributions are present: the existence of states having mutual overlap q, and their statistical weights. Therefore to have a non zero value of P for a certain overlap q, it is necessary first of all that there are some pure states which have mutual overlap q, but also that the global statistical weight of all these states is relevant in the thermodynamic limit.

If one computes $P(q)$ for the p-spin spherical model, one finds the following result.

- For $T > T_s$, when the RS solution is the one which gives the statics, one has

$$P(q) = \delta(q) \tag{2.10}$$

  This is a trivial result: only the value $q = 0$ has a non zero contribution. This distribution together with equation (2.6) suggests that in this range there is only one paramagnetic state of self-overlap equal to zero. This is surely what happens, for example, for the SK model in the high temperature phase. However, as we shall see in the next section and how the presence of metastable states above T_s indicates, this interpretation is not true for the p-spin spherical model.

- For $T < T_s$, when the good solution is the RSB one, the overlap distribution is

$$P(q) = x \ \delta(q) + (1 - x) \ \delta(q - q_1) \tag{2.11}$$

  where x and q_1 are the same variational parameters that appear in the RSB solution. In this case there are two non zero contributions: one for $q = 0$ and one for $q = q_1$. This means that the possible values of the overlap are at least two and correspond to a situation in which many pure states are present, having self-overlap equal to q_1 and mutual overlap equal to 0. The parameter x modules the balance between the probability of picking up twice the same state, and the probability of picking up two different states. It has therefore a clear statistical interpretation, and cannot be greater than one otherwise $P(q)$ would be ill defined. This is consistent with the fact that for $T > T_s$, when x becomes greater than one, the RSB solution does not give the statics any more.

As T approaches T_s from below, q_1 increases, tending to a value which remains smaller than one, while x increases and becomes equal to one at the transition. In terms of $P(q)$ this means that the delta function in q_1 has a weight which is lower and lower as the transition is nearer, and becomes vanishing at T_s. This suggests that above T_s the contribution of the self-overlap is not present not because there are not states with self-overlap q_1, but because the probability of picking up twice one of them has become vanishing.

3. The TAP approach

The TAP (Touless, Anderson, Palmer) approach [25] consists in formulating self-consistent mean-field equations for the local magnetizations $m_i =< \sigma_i >$, for fixed values of the couplings J, that is for a given sample. For the p-spin spherical model the TAP equations were first formulated in [21], where the authors gave an expression for a TAP free energy f_{TAP} [31], function of the m_i, by minimizing which one can recover the equations for the magnetizations. More recently these equations have also been directly derived with the cavity method [2,30].

The TAP equations are better analyzable if we express the magnetization vector m in terms of its angular part $\hat{\sigma}$ and of its self-overlap q:

$$m_i = \sqrt{q}\,\hat{\sigma}_i \qquad \hat{\sigma}\cdot\hat{\sigma} = \sum_i \sigma_i^2 = N \ . \tag{3.1}$$

In this way the TAP equations for the $\hat{\sigma}_i$ read

$$0 = -p \sum_{i_2<\ldots<i_p} J_{k,i_2\ldots i_p}\,\hat{\sigma}_{i_2}\ldots\hat{\sigma}_{i_p} - pE(\hat{\sigma})\,\hat{\sigma}_k \quad , \quad k = 1,\ldots,N \tag{3.2}$$

where $E(\hat{\sigma})$ is the zero temperature energy density

$$E(\hat{\sigma}) = -\frac{1}{N}\sum_{i_1<\ldots<i_p} J_{i_1\ldots i_p}\hat{\sigma}_{i_1}\ldots\hat{\sigma}_{i_p} \ . \tag{3.3}$$

The TAP equation for q read

$$\beta q^{\frac{p}{2}-1}(1-q) = z \tag{3.4}$$

with

$$\begin{aligned} z &= (p-1)^{-1}\left[-E \pm \sqrt{E^2 - E_{th}^2}\right] \\ E_{th} &= -\sqrt{\frac{2(p-1)}{p}} \end{aligned} \tag{3.5}$$

.

where the *threshold* energy E_{th} is a maximum value for the energy density above which the equation for q has no more solution.

One can see that the equations (3.2) do not depend on the temperature, while the equation for q does. This means that the dependence on temperature of a certain solution comes entirely from q, while the behaviour with respect to the angular variables is identical to the one at zero temperature. Thus each zero temperature solution $(\hat{\sigma}_\alpha; q = 1)$ is continuously mapped into a corresponding solution $m_\alpha(T) = \hat{\sigma}_\alpha \sqrt{q_\alpha(T)}$ at temperature T, until a maximum value T_α of the temperature above which the equation for q_α has not solution anymore. There is no merging, nor splitting of solutions and one can also show that there is no chaos with respect to the temperature: the ordering in energy between two solutions at temperature T is the same as the ordering of the corresponding solutions at zero temperature.

If we solve the TAP equations at $T = 0$ we find that there is an exponentially high number of solutions all having energy density included in a finite range $[E_{min}, E_{th}]$. Moreover for each energy density E in this range there is an exponentially high number of solutions all having that energy:

$$\mathcal{N}(E) = e^{N\Sigma(E)} \ . \tag{3.6}$$

The quantity $\Sigma(E)$ is called *complexity* or *configurational entropy* [14,32] and can be explicitly computed in various ways [26,22]. It is a sort of entropy related to the presence of many states all having the same energy density. It turns out that $\Sigma(E)$ is a continuous increasing function, which is zero for the ground solutions and reaches a finite maximum value for the threshold solutions. This means that the solutions with the lowest energy are of order N and are qualitatively much less numerous than all the others, while the solutions with the highest energy are the ones entropically dominant.

At a finite temperature T, due to the mapping of the solutions, the frame is identical to the one at zero temperature. To each value of the zero temperature energy density E corresponds a free energy density $f(E,T)$. There will be $\mathcal{N}(f) = \exp(\Sigma(f))$ solutions each one having the same free energy density f, with $\Sigma(f(E,T)) = \Sigma(E)$.

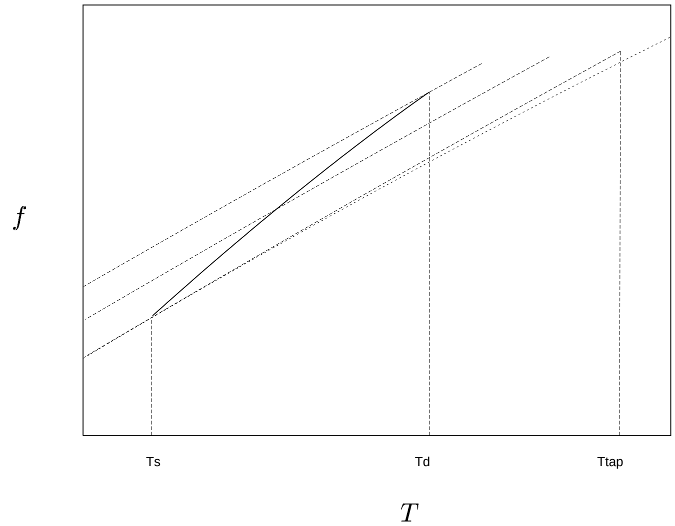

Figure 1-1: The free energy density of the TAP solutions as a function of the temperature. Three solutions are followed from T=0 until their ending temperature T=T_{TAP}, they are: the lowest solution with E=E_{RSB}, an intermediate solution, and the highest solution with E=E_{th}. The dark line is the equilibrium line $\dot{\phi}$=0, the dotted line is the paramagnetic solution.

Figure 1-1 resumes the whole description, showing the dependence on temperature of the TAP solutions. One can see that the solutions form a sort of energetic strip which evolves with the temperature. The low dotted line represents the paramagnetic solution $m_i = 0$. The threshold solutions are the first to disappear, while the lowest solutions are the latest: at the temperature T_{TAP} there are no more TAP solutions, except the paramagnetic one.

From this figure it appears clearly that for $T < T_{TAP}$ the system exhibits a huge number of solutions. Each solution corresponds to different values for the local magnetizations and therefore identifies a different pure state. In this context, the system is not ergodic and its partition function is then given by

$$Z = \sum_{a=1,\ldots\mathcal{N}} Z_a = \sum_{a=1,\ldots\mathcal{N}} e^{-\beta N f_a} \tag{3.7}$$

where Z_a is the partition function of the pure state a. Equation (3.7) can also be written in terms of the number $\mathcal{N}(f)$ of solutions with free energy density f:

$$\begin{gathered} Z = \int df \mathcal{N}(f)\; e^{-\beta N f} = \\ \int df\; e^{-\beta N(f - T\Sigma(f))} = \int df\; e^{-\beta N \phi(f)} \end{gathered} \tag{3.8}$$

where $\phi(f)$ is a sort of generalized free energy, which takes into account both the free energy contribution of each individual solution, and the entropic contribution due to the presence of many solutions all with the same free energy density. In the thermodynamic limit one can use in (3.8) the saddle point approximation: the integral is then given by the dominant contribution, that is by the value f_{eq} which minimizes the generalized free energy ϕ. Therefore the free energy density of the system is

$$F = -\frac{1}{N\beta} \log Z = f_{eq} - T\Sigma(f_{eq}) \; . \tag{3.9}$$

This means that, at a given temperature T, there is a class of solutions, the ones with free energy density f_{eq}, which dominates over all the others and gives the equilibrium properties of the system. All the other solutions do not contribute to the thermodynamics. We note that all the TAP solutions, for $T > T_s$, correspond to pure states with vanishing individual thermodynamical weight:

$$w_a = \frac{e^{-\beta N f}}{Z} = \frac{e^{-\beta N f}}{e^{-\beta N (f_{eq} - T\Sigma(f_{eq}))}} = e^{-\beta N (f - f_{eq} - T\Sigma(f))} \to 0 \tag{3.10}$$

This is valid also for the equilibrium solutions since in this case (3.10) becomes $w_{eq} = \exp(-N\Sigma(f_{eq}))$ which vanishes in the thermodynamic limit. Therefore each equilibrium solution, singularly considered, is not thermodynamically relevant: it is the collective contribution of the whole class of equilibrium solutions which is relevant.

At different temperatures the class of equilibrium solutions is in general different. The dark line in figure 1-1 is the line $\dot{\phi}(f) = 0$ that gives for each value of the temperature the equilibrium value $f_{eq}(T)$. One can see that this equilibrium line intersects the strip of TAP solutions in two points: the first point is at the static transition temperature T_s, and the second one is at the dynamical transition temperature T_d. For

$T_s < T < T_d$ the equilibrium line is in correspondence of a class of TAP solutions and thus individuates the dominating equilibrium solutions. The equilibrium value f_{eq} decreases with decreasing the temperature and for $T = T_s$ the equilibrium solutions are the ones with lowest free energy density. These solutions have zero complexity and from (3.10) we can see that they have a finite thermodynamical weight. For $T < T_s$ the minimization of $\phi(f)$ would bring to non existing solutions with $f < f_{min}$, therefore the class of dominating solutions remains the one with the lowest f and finite weight. Also for $T > T_d$ the line $\dot{\phi}(f) = 0$ would correspond to non existing solutions, this time with $f > f_{th}$. What happens is therefore that the dominating solution becomes the paramagnetic one, whose free energy density is, for $T > T_d$, lower than the generalized free energy of all the classes of non trivial TAP solutions.

For what concerns the equilibrium properties of the system, we can then resume all what said above in the following scheme. There are three ranges of temperatures in which the equilibrium behaviour of the system is qualitatively different:

- For $T < T_s$ the system is dominated by the solutions with the lowest free energy density. These solutions are finite in number, and each of them has a finite individual weight. This situation is very similar to what happens in the low temperature phase of models with continuous transition.

- For $T_s < T < T_d$ the equilibrium solutions have $f_{eq} > f_{low}$ and are in an exponentially high number. This phase is characteristic of the models with discontinuous transition while it is not present in models with a discontinuous transition. The very reason for which such a behaviour is possible is that there are so many states with f_{eq} that, when considering their entropic contribution, they result dominant even if each one of them has, singularly taken, a vanishing thermodynamical weight.

- For $T > T_d$ the equilibrium solution is the paramagnetic one. This is what usually happens in the high temperature phase. However we note that in this case even if the paramagnetic solution is the dominating one, still many other TAP solutions continue to exist up to $T = T_{TAP}$.

In this context we can better understand what is the physical meaning of the static transition that takes place at $T = T_s$. A lot of pure states, of equilibrium and not, exist also for $T > T_s$, it is then evident that the transition does not correspond to an ergodicity breaking. What happens at T_s is that the statics is no longer dominated by an exponentially high number of solutions with vanishing individual weight, but the equilibrium solutions become finite and with finite individual weight. This phenomenon is usually called *entropy crisis*, referring to the fact that the configurational entropy $\Sigma(f_{eq})$ becomes zero at the transition, and remains null in the low temperature phase [7,11].

Given the richness of states present in this model, we would like at this point to precise some notions that we shall often use in the future. Usually one indicates as 'stable states' the ones which have the lowest free energy density, in our case these states correspond to the lowest TAP solutions. All the pure states with higher free energy density are called 'metastable'. Often the stable states are also the equilibrium ones, that is the states which dominate the partition function. This is not the case in our model since, as we have seen, in the intermediate range the dominant TAP solutions are not the lowest ones and therefore correspond to metastable states. Given a certain temperature T we shall often use 'local equilibrium states' to indicate all those states, both stable and metastable, which are not the equilibrium ones at that temperature.

4. A comparison between the Replica and the TAP approach

With the TAP approach it is possible to point out the presence of many states and to compute the free energy density F of the system in terms of the free energy density f_{eq} of the individual dominating states and their entropic collective contribution $\Sigma(f_{eq})$. In the replica approach, on the other hand, one directly computes the global free energy density F of the system grace to the replica trick. It is clear that, to be consistent, the two methods must give the same results. This is actually what happens, but it is not so evident.

- For $T < T_s$ in the TAP approach the dominating solutions are the lowest ones which have zero complexity. Therefore the free energy of the system is:

$$F = \phi(f_{eq}) = f_{min} \tag{4.1}$$

  In the same temperature range the Replica approach provides a replica symmetric broken solution and gives

$$F = F_{RSB} \tag{4.2}$$

  where F_{RSB} is the one given in (2.7). If we look at the TAP equations and imposes $\Sigma(f) = 0$ we can simply get an explicit expression for f_{min}. It turns out that this expression is identical to (2.8), and the variational parameter q_1 identifies with the self-overlap q_{min} given by the TAP equations.

- For $T_s < T < T_d$ the situation is less clear. The Replica approach provides a replica symmetric solution and gives;

$$F = F_{RS} = F_{para} \ . \tag{4.3}$$

  On the other hand the TAP approach says that the equilibrium is given by a bunch of exponentially numerous different solutions and this seems to be inconsistent with the replica result. Luckily what happens is that the whole contribution of all the equilibrium solutions is exactly equal to the contribution of the single paramagnetic solution so that, for what concerns the free energy of the system one has:

$$F = \phi(f_{eq}) = f_{eq} - T\Sigma(f_{eq}) = F_{para} \ . \tag{4.4}$$

  Therefore the two methods turn out to be consistent also in this temperature range.

- For $T > T_d$ both the methods give explicitly $F = F_{para}$ and there are no ambiguities.

From this comparison we can deduce some important things about the interpretation of the replica solutions. Usually one is led to think that an RS solution corresponds to the paramagnetic state. We have just seen that this is not always true. What happens is that a replica symmetric solution is indeed compatible with two very different situations: the first is when the statics is given by a single paramagnetic state, as for $T > T_s$; the second is when there is an exponentially high number of dominating states, as for $T_s < T < T_d$. On the other hand an RSB solution corresponds to the situation in which there are many states giving the statics and not only one, but these states are not exponentially high in number.

5. Information on the structure of the states

After this overview on the statics of this model, we would like to focus about the principal subject of this thesis, that is the structure of the states in the phase-space, and show what the TAP and the Replica approach can tell about it.

The TAP approach has the great advantage of describing the system in terms of all its states. It provides an exact knowledge of the free energy density, the energy density and the self-overlap of each individual solution. One can obtain these properties directly from the TAP equations and not only for the equilibrium solutions which dominate at a certain temperature, but also for all the other solutions which are not of equilibrium. Unfortunately nothing is said on the mutual distances between different solutions, of the same or of different classes.

The Replica approach describes the global equilibrium behaviour of the system, and all the information it gives on the states is contained in the overlap distribution $P(q)$ previously introduced. We can now try to reinterpret this distribution, in the light of what understood in the last sections.

For $T > T_s$ the $P(q)$ is a delta function in zero. It is evident that for $T > T_d$ this shape has to be associated to the paramagnetic dominant state: in this case there is only one equilibrium state with self-overlap $q = 0$, while all the other states even if present are not thermodynamically relevant and therefore do not give any contribution to the $P(q)$.

Between T_s and T_d the question is more subtle, indeed we now know that in this temperature range the equilibrium states are many and with self-overlap different from zero. In this situation we expect a contribution to the overlap distribution of the self-overlap of the dominant states, as it happens below T_s. Yet in this range the $P(q)$ still is a delta on zero and has not this contribution. The reason for that becomes clear if one reminds the definition of this distribution: $P(q)$ is the probability that, picked up two states, their mutual overlap is equal to q. In this range, as we now, the equilibrium states are exponentially numerous and have, singularly taken, a vanishing weight in the thermodynamical limit. For what concerns $P(q)$ this means that, both for a purely entropical reason and because of the small weight, it is highly unlikely to pick up twice the same state and measure its self-overlap: this value of the overlap has a vanishing probability when $N \to \infty$. More precisely, from equation (2.9) we can deduce the contribution of the self-overlap of the equilibrium states, which is $P(q_{EA}) = \sum_{eq} w_{eq}^2$, and express it in terms of TAP solutions to obtain

$$\sum_{eq} w_{eq}^2 = \sum_{eq} \frac{e^{-2\beta N f_{eq}}}{Z^2} = \frac{e^{-\beta N(2f_{eq}-T\Sigma(f_{eq}))}}{e^{-2\beta N(f_{eq}-T\Sigma(f_{eq}))}} = e^{-N\Sigma(f_{eq})} \tag{5.1}$$

that vanishes for $N \to \infty$.

In this way we have explained why there is not a contribution at the self-overlap, but it still remains to understand what the delta function in zero says of the mutual overlaps between different states. One possibility is certainly that *all* the states of the system are at mutual overlap equal to zero, and thus $q = 0$ is actually the only possible value for the overlap between two different states. But there is also another possibility. Maybe the $P(q)$ does not catch a contribution from all the other possible values of the overlap q, not because states with mutual overlap q do not exist, but, as in the case of the self-overlap, for probabilistic reasons: the states with mutual overlap different from zero are not enough numerous so that the probability of picking up two of them vanishes in the thermodynamic limit.

For $T < T_s$ the situation is surely simpler to interpret. In this range the equilibrium states are the lowest stable ones, have finite weight and are finite in number. The $P(q)$ has two deltas, one in zero and one at the self-overlap: indeed the contribution of the self-overlap as given in (5.1) does not vanish anymore since in this case $\Sigma(f_{eq})$ is zero. For the stable states then both $q = 0$ and $q = q_{EA}$ are values probabilistically possible, the first corresponding to the overlap between two different states, and the second corresponding to the self-overlap of each of them.

We must then conclude that the overlap distribution $P(q)$ obtained in the standard replica approach, which turns out to be trivial in the intermediate temperature range, does *not* provide a clear information on the structure of the states, because it is compatible with two very different scenarios:

i) In the first one the trivial $P(q)$ corresponds to a structure which is itself trivial with *all* the states having mutual overlap equal to zero.

ii) In the second one there is a non trivial structure of the states, with mutual overlap different from zero, which is not revealed by the $P(q)$ for probabilistic reasons.

The starting point of most of the work exposed in this thesis was the conviction that there were indeed too many states to reasonably think that they all had mutual overlap equal to zero. Thus the second scenario was believed to be the right one: with this opinion some non standard methods have been developed, to reveal the hidden non trivial structure of the states and investigate it.

6. The dynamical behaviour and the role of threshold states

The asymptotic dynamics of this model can been analytically solved [9,10,12,4], and reveals a very special role played by the threshold states. The standard analysis consists in considering a system which starts from a random initial configuration and assume for it a Langevin relaxational dynamics. One then sets $N \to \infty$ from the beginning and studies the behaviour of the system for diverging times. With standard functional methods the dynamical equations for the correlation and the response functions can be obtained. These equations can be solved both in the high and in the low temperature phase and show the following scenario:

- For $T > T_d$ the system exhibits an equilibrium asymptotic dynamics in which the time translation invariance and the fluctuation dissipation theorem hold. The correlation function $C(t-t') = \overline{s(t) \cdot s(t')}$ decays exponentially to zero, i.e. to the self-overlap of the paramagnetic state which in this range determines the statics. When T approaches T_d still the dynamics is of equilibrium, but the behaviour of the correlation function changes: there is a first power law decay towards a plateau given by the self-overlap of the threshold states, and a second power law decay towards zero. The time spent on the plateau is finite as long as T is different from T_d and diverges at the dynamical transition. This behaviour is very similar to the one obtained in the context of the Mode Coupling Theory for super-cooled liquids, and the dynamical equations are indeed analogous [13,16].

- For $T < T_d$ the system exhibits an off-equilibrium dynamics in which the time translational invariance and the fluctuation-dissipation theorem in general does not hold. Therefore both the response and the correlation function depend on two times, this implying aging. Actually one can distinguish two time regimes in which $C(t,t')$ behaves in a different way. Let us imagine to observe the system from a certain (very big) waiting time t' and to look at its evolution at time $t > t'$. For $t - t'$ small the correlation function depends only from $t - t'$ and decays as a power low towards a plateau given by q_{th}. It remains on the plateau for a diverging time of the order of t' and as $t - t'$ becomes big decays slowly to zero with a decay rate which depends on the waiting time t'. The asymptotic energy reached by the system is $\lim_{t\to\infty} E(t) = E_\infty = E_{th}$, i.e. the energy density of threshold states.

The interpretation of the low temperature dynamics is still rather unclear. The system starts from a high energy configuration and relaxes towards the threshold level, as indicated by the value of the asymptotic energy, never visiting the sub-threshold landscape. The system explores a region of the phase space which corresponds to a threshold state, since the plateau is exactly at q_{th}. However it never truly thermalizes into this state, but rather continuously drifts away as the decay to zero of the correlation function indicates. The physical reasons of this behaviour are not well understood, even if various explanations have been proposed [33,34,35,4]. What is clear is that for $T < T_d$ the asymptotic dynamics is determined by the threshold states, even when these states are not statically relevant. It is therefore intriguing to discover what are the properties which make these states so important.

Surely a crucial point is that the threshold states are *marginal*: the typical spectrum of the TAP Hessian in a solution of energy density E is a semi-circle with support on the positive semi-axis, and its lowest eigenvalue goes to zero as E approaches E_{th}. This means that threshold states develop some flat directions and in this sense are called marginal.

Another point that is worth to investigate is the geometrical structure of the threshold states in the phase space: maybe these states are disposed in a very special way which can be related with their dynamical role. We shall see in the next chapters that this is indeed the case.

Chapter II: The Real Replica method

In the previous chapter we have shown that the standard statical methods fail in giving a clear view of the structure of the states in the p-spin spherical model. More precisely the only available information on this topic remains quite ambiguous, since it leaves open two very different possibilities: the first one consists in a trivial structure with all the states orthogonal one with respect to the other, while the second one provides for a hidden non trivial structure with states having mutual overlap also different from zero. The problem is therefore to develop some methods which are able to distinguish between these two scenarios, and, in the more interesting case of a non trivial structure, are able to investigate it.

The Real Replica method is one of these methods and mainly consists in the statical analysis of a system subjected to some external constraints [21][22,36][37,38] [23,24]. It lies in the general context of the Replica method, since its strategy is to compute the free energy of the constrained system using the replica trick.

We have seen that the p-spin model is characterized by the presence of many pure states. In such a situation the system is not ergodic and the Boltzmann measure splits into a sum of ergodic measures, each one corresponding to a different pure state. All the thermo-dynamical averages obtained with the Boltzmann measure are therefore averages over *all* the states. When performing a standard statical analysis with the Replica Method one directly computes the free energy of the system as an average over the Boltzmann measure and thus what one finally obtains is a total free energy, which takes into account the contributions of all the equilibrium states, without distinguishing among them.

From what said above it is clear that the only way in which, within this method, it is possible to study the properties of an individual state is to use a measure which reproduces only the contribution of that single state. This purpose can be pursued by studying a constrained system. Indeed in this case the system, because of the constraints to which it is subjected, cannot visit all the phase space and is forced to thermalize in a restricted region of it. In this way, opportunely varying the constraints, one can induce the system to thermalize into a single pure state.

A first application of this method can be, for example, the following. One considers two or more identical copies (Real Replicas) of the system, and imposes a certain fixed overlap q between them. The free energy of this composite system will depend on q and can give interesting information on the free energy landscape of the *free system*. For general values of the overlap q the replicas will be in a region of the phase space which does not correspond to anything sensible for the free system. But if, for example, q

is equal to the self overlap of a certain metastable state and the number of coupled replicas is opportunely chosen, they will find their equilibrium just in that zone of the phase space which correspond to that metastable state. This analysis has been performed in [21], and, in a more general fashion in [39].

A different strategy, which is the one we will develop in the following, is that of the so-called Potential method. In this case one fixes one or more equilibrium configurations in the phase space and consider a system which is forced to have certain overlaps with those configurations. The free energy of the constrained system, the effective potential function, depends on the imposed overlaps and one can explore with it the phase space around the fixed configurations.

1. The two-replica potential

The simplest case in which the Potential method has been applied is the one of the two-replica potential that we shall discuss in details in this section [22,37,38].

Let me consider two systems both having the Hamiltonian of the p-spin spherical model, and call them, respectively, replica 1 and replica 2. The first system (replica 1) is freely thermalized at a certain temperature T in the range $T_s \leq T \leq T_d$. Then an equilibrium configuration σ of this system is extracted and fixed as a reference configuration in the phase space. The equilibrium of a free system is in this range given by a bunch of dominant pure states and the configuration σ thus belongs to one of them: in this sense fixing σ as reference point in the phase space means also to fix one of the numerous equilibrium states of replica 1. Once fixed the configuration σ, the second system (replica 2) is forced to thermalize keeping a certain overlap q_{12} with the reference configuration.

The two real replicas that we have introduced have a very different role: replica 1 indeed thermalizes according to the canonical Boltzmann distribution and has all the statical properties treated in Chapter I; replica 2, on the other hand, thermalizes following a constrained distribution which strictly depends on replica 1, and its statics will be different with respect to the one of a free system.

The two-replica potential is defined as the free energy cost payed to keep the constrained system (replica 2) at a fixed overlap q_{12} with the reference configuration σ (replica 1):

$$V_2(q_{12}) = F_{const}(q_{12}) - F_{free} \tag{1.1}$$

where F_{free} is the free energy density of a free system. The more replica 2 is forced to thermalize in a way that is out of equilibrium for the free system, the more one has to pay. Vice versa the minima of the potential $V_2(q_{12})$ with respect of q_{12} correspond to the case in which the constrained system has found a situation of local equilibrium of the free system (see Appendix 2-A). Therefore one must look at the minima of the potential since these minima correspond to stable or metastable states of the free system. Indeed this is the general strategy of this method, also in the case of more complex potential functions when more than one configurations are fixed in the phase space and there is a greater number of external constraints: computing the potential and looking at its minima in the overlaps-space. The first step of my analysis will then be the computation of the two-replica potential.

2. The computation of the potential function

The explicit expression of the potential function is

$$
\begin{aligned}
&-\beta N V_2(q_{12}) = \\
&\overline{\log \left(\int d\tau \exp(-\beta H(\tau))\ \delta(q_{\sigma\tau} - q_{12}) \right)} - \overline{\log Z_{free}}\ .
\end{aligned}
\tag{2.1}
$$

We can see in (2.1) that the potential depends both on q_{12} and on the fixed configuration σ. However σ is an equilibrium configuration and this means that it can be drawn as a typical realization of the canonical Boltzmann distribution. It is reasonable to suppose that the potential function is self averaging with respect of σ, in the sense that one can average $V_2(q_{12})$ with the distribution of σ expecting that this is the same as evaluating the potential in a particular fixed realization of it. Then a successive expression for (2.1) is

$$
\begin{aligned}
&-\beta N V_2(q_{12}) = \\
&\overline{\frac{1}{Z_{free}} \int d\sigma \exp(-\beta H(\sigma))\ \log \left(\int d\tau \exp(-\beta H(\tau))\ \delta(q_{\sigma\tau} - q_{12}) \right)} \\
&\qquad - \overline{\log Z_{free}}\ .
\end{aligned}
\tag{2.2}
$$

It is important to note that the two integrations which appear in equation (2.2) are related to two very different things. The integration over the variable σ indeed represents the *annealed* average that one operates on the equilibrium distribution of replica 1. On the other hand the integration on the τ expresses the partition function of replica 2, of which one computes the free energy. There is therefore an explicit asymmetry in the integration variables which reproduces the hierarchy existing between the two real replicas.

To perform the average over the quenched disorder, we use the replica trick exploiting the two relations

$$
\begin{aligned}
\log Z_{const} &= \lim_{m\to 0} \frac{Z_{const}^m - 1}{m} \\
\frac{1}{Z_{free}} &= \lim_{n\to 0} Z_{free}^{n-1}\ .
\end{aligned}
\tag{2.3}
$$

In this way one has

$$
\begin{aligned}
&-\beta N V_2(q_{12}) = \lim_{n,m\to 0} \frac{1}{m} \\
&\overline{\log \int d\sigma_a d\tau_b \exp\left[-\beta \left(\sum_{a=1}^{n} H(\sigma_a) + \sum_{b=1}^{m} H(\tau_b) \right) \right] \prod_{b=1}^{m} \delta(q_{\sigma_1 \tau_b} - q_{12})} \\
&\qquad\qquad\qquad - \overline{\log Z_{free}}\ .
\end{aligned}
\tag{2.4}
$$

In this expression σ_1 is the same as the coordinate σ of equation (2.2) while the other replicas σ_a; $a = 1 \ldots n$ are those which express Z_{free}^{-1}; this is the reason why the delta function of the constraint only involves σ_1.

At this point we proceed as in the computation of the free energy of a free system, but in this case the overlap matrix will be more complicated since one has to consider all the overlaps between the replicas of τ and those of σ. It is convenient to introduce the overlap sub-matrices

$$\begin{aligned} Q^{11}_{ab} &= q_{\sigma_a \sigma_b} \qquad a = 1, \ldots, n;\ b = 1, \ldots, n \\ Q^{12}_{ab} &= q_{\sigma_a \tau_b} \qquad a = 1, \ldots, n;\ b = 1, \ldots, m \\ Q^{22}_{ab} &= q_{\tau_a \tau_b} \qquad a = 1, \ldots, m;\ b = 1, \ldots, m \end{aligned} \tag{2.5}$$

and $Q^{21}_{ab} = Q^{12}_{ba}$; in this way the total matrix of the overlap $\mathbf{Q}$ formed by the blocks (2.5) is symmetric. With this definition, equation (2.4) gives

$$-\beta V_2(q_{12}) = \operatorname*{Ext}_{\mathbf{Q}} \left\{ \lim_{n,m \to 0} \frac{1}{2m} \left(\beta^2 \sum_{a,b} f(\mathbf{Q}_{ab}) + \log \det \mathbf{Q} \right) \right\} + \beta F_{free} \ . \tag{2.6}$$

Before proceeding with the calculation, it is necessary to give a sensible ansatz for the overlap sub-matrices. Q^{11} is referred to replica 1, which is an independent free system thermalized at a temperature $T > T_s$, therefore one assumes for it the symmetric form

$$Q^{11}_{ab} = \delta_{ab} \ . \tag{2.7}$$

The structure of Q^{12} is in part imposed by the constraint in (2.4), that forces the first row to be equal to q_{12}. The simplest ansatz for the whole sub-matrix is

$$Q^{12}_{ab} = q_{12}\ \delta_{a,1} \ . \tag{2.8}$$

This choice is sensible for two different reasons.

First of all this choice is compatible with an analysis in the high temperature region. At $\beta = 0$ the calculation of V_2 reduces to a purely geometrical problem; indeed, in this case the potential is simply proportional to the volume of the phase space region accessible to the constrained replica. Therefore, the comparison with this limit is useful to test the correctness of the ansatz for the overlap matrices and one can check that in the limit $\beta \to 0$ equation (2.8) gives the expected resuls.

Moreover, one can introduce an additional parameter w_{12} for the rest of the matrix and verify that, even for finite values of β, the saddle point equations lead to the solution $w_{12} = 0$: this confirms that the ansatz (2.8) is correct also in the temperature range we are interested in.

In [22] Q^{22} was assumed symmetric, but a successive examination suggested that a more general one step RSB form has to be taken [40], with variational parameters (x_r, r_1, r_0):

$$Q^{22}_{ab} = (1 - r_1)\ \delta_{ab} + (r_1 - r_0)\ \epsilon_{ab} + r_0 \tag{2.9}$$

where ϵ_{ab} is equal to one in the diagonal blocks of size x_r and zero elsewhere.

With these assumptions we obtain (see Appendix 2-B for details):

$$\begin{aligned} -2\beta V_2(q_{12}) = \underset{r_0,r_1,x_r}{\mathrm{Ext}} \Bigg\{ & 2\beta^2 f(q_{12}) + \beta^2(x_r-1)f(r_1) - \beta^2 x_r f(r_0) \\ & + \log(1-r_1) + \frac{1}{x_r}\log\left(1+x_r\frac{r_1-r_0}{1-r_1}\right) + \frac{r_0-q_{12}^2}{1-r_1+x_r(r_1-r_0)} \Bigg\} . \end{aligned} \tag{2.10}$$

The parameters with respect to which the potential has to be maximized are (x_r, r_1, r_0) and the saddle point equations read:

$$\begin{aligned} (1-x_r)\beta^2 f'(r_1) &= (1-x_r)\ \frac{1}{(1-r_1+x_r(r_1-r_0))^2}\left(r_1-q_{12}^2+x_r\frac{(r_1-r_0)^2}{1-r_1}\right) \\ x_r\beta^2 f'(r_0) &= x_r\ \frac{(r_0-q_{12}^2)}{(1-r_1+x_r(r_1-r_0))^2} \\ \beta^2 f(r_1) - \beta^2 f(r_0) &= \frac{1}{x_r^2}\log\left(1+x_r\frac{r_1-r_0}{1-r_1}\right) \\ & \qquad - \frac{1}{x_r}(r_1-r_0)\ \frac{1-r_1+x_r(r_1-2r_0+q_{12}^2)}{(1-r_1+x_r(r_1-r_0))^2} . \end{aligned} \tag{2.11}$$

It is possible to solve numerically these equations, the resulting $V_2(q_{12})$ is shown in figure 2-1.

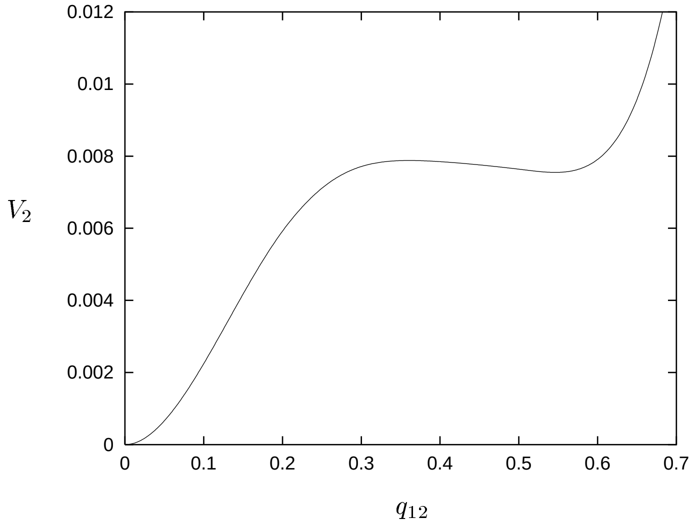

Figure 2-1: The potential V_2 as a function of q_{12} at β=1.64 and p=3; q_{EA}=0.546.

3. The minima of the two-replica potential

How we said at the beginning of this chapter, the important things to look at are the minima of the potential function, since these minima correspond to local or global equilibrium situations of the free system.

In the case of the two-replica potential, as one can see from figure 2-1, there are two minima:

i) There is an absolute minimum for $q_{12} = 0$, that is with replica 2 orthogonal to replica 1. In this minimum one has $V_2 = 0$, and thus the cost to keep replica 2 at overlap zero with the pure equilibrium state of replica 1 is null. This means that when $q_{12} = 0$ the constrained system actually thermalizes as a free system. Indeed for $q_{12} = 0$ the phace space accessible to replica 2 is a $N-1$ dimensional sphere, thus in thermodynamical limit replica 2 see a phase space identical to that of a free system. This is not a surprise. We have shown in Chapter I that the overlap distribution $P(q)$ of a free system has only a contribution for $q = 0$, this indicating that almost all equilibrium states are at zero mutual overlap. If we fix an equilibrium state, the most part of other equilibrium states will then be at overlap $q = 0$ with it and all the others will give a vanishing contribution. Therefore this minimum corresponds to the global equilibrium of the free system, and replica 2 thermalizes catching the contribution of all the equilibrium states orthogonal to the equilibrium state of replica 1.

ii) There is also a relative minimum M for

$$q_{12} = q_{EA} \tag{3.1}$$

where q_{EA} is the self-overlap of an individual equilibrium state, as given in the TAP approach. This minimum corresponds to the situation in which replica 2 has an overlap with replica 1 which is equal to the self overlap of the equilibrium state of replica 1: the two replicas are therefore in the same state. What happens is that highing up the value of q_{12} replica 2 is forced to thermalize nearer and nearer to replica 1, until when, for $q_{12} = q_{EA}$ it properly thermalizes into the same state of replica 1. To have a confirmation of this fact we look at the sub-matrix Q^{22} which is the one related to replica 2: indeed when the system is in a single ergodic component (as happens for a free p spin system in the paramagnetic phase) the overlap matrix is symmetric and has only one variational parameter which represents the self-overlap of the state in which the system is. It turns out that in M the sub-matrix Q^{22} is symmetric, with

$$r_0 = r_1 = q_{12} = q_{EA} \tag{3.2}$$

that is in accord with the previous analysis.

As expected the two minima of V_2 actually correspond to situations physically meaningful for the free system. The absolute minimum is trivial, in the sense that reproduces the results of the standard replica approach taking the contribution of all the equilibrium states together. The relative minimum is the new interesting result, since it corresponds to a single equilibrium state of the free system while the standard replica approach is not able to catch this individual contribution. With the two-replica potential it is then possible to study the properties of a single equilibrium state simply looking at V_2 in the minimum M. Since in this minimum replica 2 thermalizes into an equilibrium state, its constrained free energy will be equal to the free energy of this state. Remembering the definition of the potential we then have

$$f_{eq} = F_{const}(q_{EA}) = V_2(q_{EA}) + F_{free} \tag{3.3}$$

where f_{eq} is the free energy density of an equilibrium state. It is important to note that both f_{eq} and q_{EA} are equal to the values given by the TAP approach for the equilibrium solutions at temperature T, thus confirming the consistence of these two different methods. This consistence leads to another important result; indeed we have seen that the total free energy density F_{free} obtained with the plain replica approach can also be expressed in terms of TAP solutions giving

$$F_{free} = f_{eq} - T\Sigma(f_{eq}) \ . \tag{3.4}$$

A comparison between (3.4) and (3.3) shows that

$$V_2(q_{EA}) = T\Sigma(f_{eq}) \ . \tag{3.5}$$

This result has a simple intuitive explanation: in this temperature range the number of equilibrium states is exponentially high so that the probability of finding twice the system in the same state is exponentially small and is proportional to $e^{-N\Sigma(f_{eq})}$ (see equation (5.1)); therefore the free energy cost to constrain two systems in the same state is of entropic origin and will be given by the logarithm of this probability, as (3.5) says. We note that in this way the potential function catches the contribution of the self-overlap of the equilibrium states while the standard $P(q)$ does not. The reason of this fact is evident: $V_2(q_{EA})$ is nothing else than the logarithm of the distribution function in this point, divided for the size of the system. Therefore in the thermodynamic limit it remains finite whereas the $P(q_{EA})$ vanishes exponentially.

4. Temperature dependence

The results of the previous section have been obtained keeping the temperature fixed. One can then ask what happens with varying the temperature.

We have seen that in the range $T_s < T < T_d$ the equilibrium states are not always the same at every temperature, on the contrary at each different temperature the class of equilibrium states is different, how the equilibrium line of figure 1-1 shows. For what concerns V_2 this means that replica 1 is fixed in a different kind of state at different temperatures. In this way varying the temperature implies studying the properties of different kinds of states.

From what said above we can also realize what should be qualitatively the behaviour of the two-replica potential with the temperature. Since the free energy and the complexity of the dominant solutions increase with increasing T one expects that higher is the temperature greater is the value that V_2 has in the relative minimum M. Moreover at T_d the equilibrium ceases to be dominated by a class of pure states and is given by the paramagnetic solution, which has self overlap equal to zero; therefore at T_d the relative minimum M, which is related to the presence of equilibrium states with finite self-overlap and vanishing entropical weight, should disappear. On the other hand at the static transition temperature the equilibrium states have zero complexity and therefore $V_2(M)$ has to become zero. In figure 2-2 it is shown the behaviour of $V_2(q_{12})$ at various values of the temperature. The upper curve corresponds to $T = T_d$ and one can see that the minimum has become a flex point; moreover one can also show analytically that the equations for the flex are the same as the marginality condition which usually identifies the dynamical transition [22]. The lower curve corresponds to $T = T_s$ and has the secondary minimum with $V_2 = 0$, as expected.

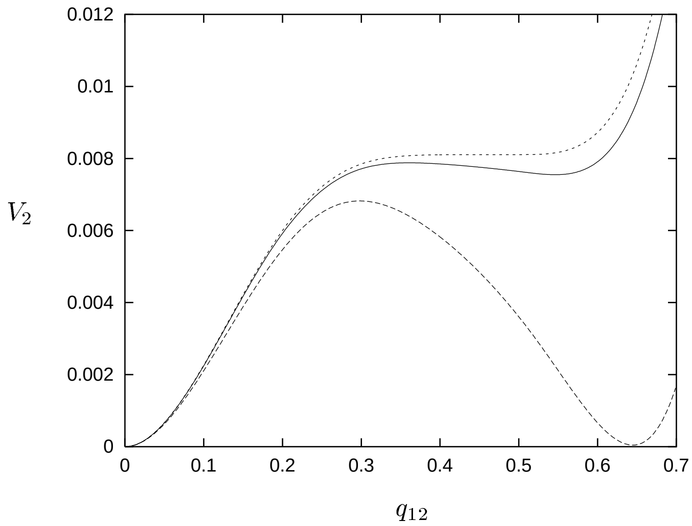

Figure 2-2: The potential V_2 as a function of q_{12} for p=3 at β=β_d=1.633 (upper curve), β=1.64 (intermediate curve) and β=β_s=1.706 (lower curve).

5. A dynamical analysis

We have seen in Chapter I that the standard dynamical analysis consists in studyind a system which starts at time zero from a random high energy configuration. In the low temperature range $T < T_d$ what one obtains is an off-equilibrium behaviour which asympotically tends to the threshold level. This is surely the most interesting situation to study since it reveals dynamical properties of this model which are very similar to those experimentally observed. However there is also a different direction one can analytically follow, which is in some sense complementare to the statical analysis of the potential method.

To this aim we now study the dynamical behaviour of a system whose initial configuration σ is not chosen at random, but is extracted following the Boltzmann distribution at temperature T. In this way the system starts its evolution in one of the numerous equilibrium states at this temperature, and we can reasonably expect that it will properly thermalize in it with a plain equilibrium relaxational dynamics. To verify this point one has to solve the equations for the dynamical quantities and look at their limiting values. In this case, besides the usual correlation function $C(t,t') = \overline{<\sigma(t)\dot{\sigma}(t')>}$, one can also consider the additional correlation function $C(t,0) = \overline{<\sigma(t)\dot{\sigma}>}$ which measures how much the system is far from the initial configuration. One finds [22,41] that actually the dynamics is of equilibrium $(C(t,t') = C(t-t') = C(\tau))$ and that the asymptotic values of $C(\tau)$ and $C(t,0)$ satisfy a set of coupled equations identical to the statical equations for $r_1 = r_0$ and q_{12} in the minimum M of the two-replica potential. Therefore one has

$$\begin{aligned} &\lim_{\tau\to\infty} C(\tau) = r_1(M) = q_{EA} \\ &\lim_{t\to\infty} C(t,0) = q_{12}(M) = q_{EA}\ . \end{aligned} \tag{5.1}$$

Equations (5.1) say that the system relaxes into an equilibrium state ($C(\tau) \to q_{EA}$ and that this state is precisely the same in which the system started its evolution ($C(t,0) \to q_{EA}$). This conclusion is enforced by the asymptotic behaviour of the dynamical energy $E(t)$, which relaxes towards the value E_{eq} of the equilibrium states, as given in the statical calculations.

It is very interesting to find in a dynamical approach exactly the same equations obtained with the statical method of the potential function. In a certain sense this is not surprise, since there are many analogies in the procedures adopted respectively in the two cases: the initial configuration of the evolving system is chosen with the same criterion with which replica 1 is fixed in the two-replica potential, while the configuration $\sigma(t)$ of the evolving system represents a sort of dynamical version of replica 2.

However we note that there is a fundamental difference between the two approaches. With the potential function we can study the constrained system for each value of q_{12}, since this overlap is an external parameter that we can change as we like. On the other hand in the dynamical approach one has not any imposed constraint and the asymptotic distance from the initial configuration is automatically given by the dynamics.

6. The two-replica potential and the structure of metastable states

The two-replica potential is surely an interesting development of the Replica approach, and is able to see things that were not revealed by the standard replica procedure: it gives the properties of the individual equilibrium states, evaluates the complexity and individuates the dynamical transition at the temperature where firstly the secondary minimum appears. However one has to admit that the information gathered on the structure of the states is actually very poor. The two minima of V_2 correspond, respectively, to the set of equilibrium states orthogonal to replica 1 ($q_{12} = 0$) and to the single equilibrium state of replica 1 ($q_{12} = q_{EA}$), nothing is said about eventual metastable states at overlap different from zero with replica 1. The ambiguity if these states actually exist or not still remains and any new step is made in this direction.

It is important at this point to understand why the two-replica potential may fail in revealing the eventual structure of the states. The main reason is that V_2 performs a radial analysis of the phase space with respect to the fixed reference replica, and this may be not sufficient to signal the presence of eventual states. To show why this can happen let us hypothesize that there are indeed states at a certain overlap $q_{12} \neq 0$ with replica 1. We know that the only way in which a potential function can individuate a state of the free system is by forming a minimum. But if there are other states with overlap immediately greater and immediately smaller than q_{12}, V_2 will not in general make a minimum in correspondence of q_{12}, in spite of the fact that these states exist. This is a problem with a radial exploration: states which are very far in the phase space, but have similar overlaps with the reference point, are seen by the the two-replica potential as nearby states with respect to q_{12}; in this way given a state at overlap q_{12} it is sufficient that somewhere in the phase space another state with $q_{12} \pm \delta\, q_{12}$ exists and this state will not be signaled by the two-replica potential. The way out for this problem will be shown in the next chapter, but it appears since now clear that one has to impose more constraints to the system, for example fixing more configurations, so that the domain of the potential function becomes a more refined projection of the phase space.

Finally, there is another point that we want to discuss. When computing the two-replica potential we have assumed for the sub-matrix Q^{22} a one step replica symmetry broken solution, as given in (2.9). However there are values of q_{12} in which this solution merges with a symmetric one and there are ranges in which the RS solution has to be considered. More precisely what happens is the following: for small values of q_{12} the RSB solution gives a value of x_r which is greater than one, and has to be discarded. At a certain value $q_{12} = q_{rsb}$, x_r becomes equal to 1 so that the RSB solution, which provides a better free energy, can be taken. There is another value of $q_{12} < q_{EA}$ for which r_0 becomes equal to r_1 so that the RSB solution recovers the RS one. This mechanism is smooth with respect of the potential function, so that from the behaviour of V_2 one cannot even understand that a replica breaking has taken place. It is not the same if one looks at the energy of replica 2.

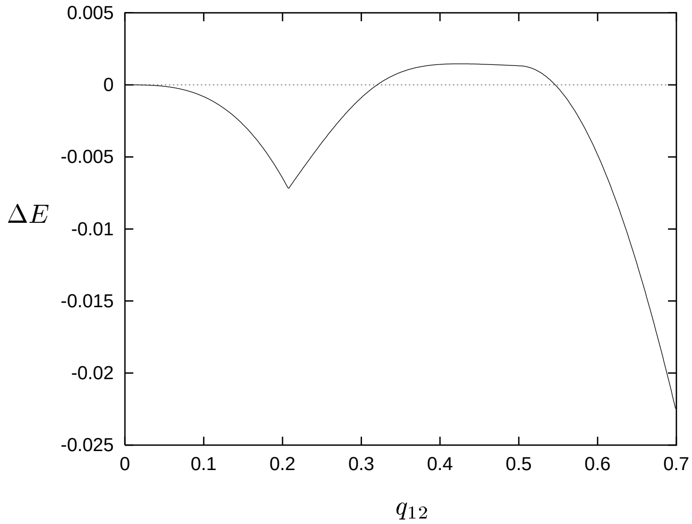

Figure 2-2: The energy density difference $\Delta E = E_{const} - E_{free}$ as a function of q_{12} at β=1.64 and p=3; q_{EA}=0.546.

In figure 2-3 the energy of the constrained system as a function of q_{12} is shown: one can see that there is a cuspid in correspondence of $q_{12} = q_{rsb}$ indicating that for this value of the overlap there is a change of solutions. On the other hand nothing happens when the solutions becomes again symmetric, since in this case it is the RSB solution which itself becomes symmetric.

One can ask if there is a physical interpretation of this behaviour. We have argumented in the first chapter what is usually the meaning of the RS and the RSB solutions: an RS solution can be related or to a single dominant pure state or to the presence of an exponentially high number of equilibrium pure states, an RSB solution on the other hand is related to a finite number of dominant pure states. This is what in general happens for a free system, but it is reasonable to guess that also in the case of a constrained system this interpretation should be true. In the case of the two-replica potential there is a system, replica 2, which has to thermalize at overlap q_{12} with the fixed configuration. Replica 2 is then forced on the manifold defined by fixing q_{12} and generally thermalizes differently for a free system. However one can argue that the mechanism of thermalization remains the same: as a free system thermalizes catching the contribution of those states which dominate in all the phase space, in the same way if there are states at overlap q_{12} with replica 1, replica 2 will thermalize catching the contribution of the dominant among these states. In this context one can easily interpret the RSB and the RS solution:

- For $q_{12} = 0$ the constrained system thermalizes as a free system, catching the contribution of an exponentially high number of states, so that the correct solution for Q^{22} must in this case be the symmetric one.

- For values of $q_{12} \neq 0$ replica 2 has access only to a restricted region of the phase space, however if q_{12} is not too high this region is quite big and one can expect that the states present in this region are still exponentially numerous, so that the correct solution continues to be the RS one.

- When q_{12} becomes equal to q_{RSB} the accessible region to replica 2 is not enough big any more and the dominant state inside it are not exponentially numerous. Therefore the correct solution for Q^{22} becomes the RSB one.

- When q_{12} becomes too high, the accessible region to replica 1 becomes just the phase space around the equilibrium state of replica 1: there will be just one dominant state in it, the one of replica 1. In this case the right solution is again the RS one.

Resuming, one can then say that at small values of q_{12} (that is at big distances from replica 1) the constrained system sees a very big number of dominant states, while at a certain value of the overlap it ceases to see an exponentially high number of equilibrium states and its constrained equilibrium is dominated by a finite number of states. This scenario of course is grounded on the hypothesis that the states are distributed in the whole phace space and are not present only at overlap equal to zero with replica 1. If this is true there is also another reason for which the two-replica potential is not good to investigate the structure of the states: in the statics of a free system one does not accede to the properties of the individual equilibrium states because the system equilibrates catching their collective contribution on the whole, exactly in the same way replica 2 does not give information on the individual dominant states at overlap q_{12} because it equilibrates in the manifold fixed by q_{12} catching the collective contribution of all the dominant states in this manifold. This indicates that the only constraint q_{12} is evidently not enough to force the system into one state and, if one wants to persist in using this approach, more constraints have to be introduced. In the next chapter a natural generalization of the two-replica potential is introduced, in which two configurations are fixed in the phase space and a third system is forced to thermalize keeping given overlaps with these two configurations. We will see that, finally, this more complicated context is enough refined to reveal the structure of the states.

Appendix 2-A

In this appendix we shall justify the reason why the minima of a potential function correspond to global or local equilibrium states of the free system.

I will consider the simplest case of the two-replica potential, even if the same reasoning can actually be performed also for more complicated potential functions.

There are two different ways of introducing the potential function $V_2(q_{12})$. The first is the one followed in this chapter and consists in considering a system which is forced to stay at overlap q_{12} with a fixed configuration. Alternatively, one can consider a system which is subjected to an attractive coupling with the fixed equilibrium configuration. In this case the global Hamiltonian will be

$$\mathcal{H}(\tau) = \mathcal{H}_{free}(\tau) - \epsilon q_{\sigma\tau} \qquad (2-\mathrm{A}.1)$$

where σ is the reference configuration and the parameter ϵ fixes the strength of the additional interaction term. This system feels the presence of the external field ϵ and thermalizes following the distribution defined by the Hamiltonian (2-A.1). If one computes the free energy of this system what one obtains will be a function $\Gamma(\epsilon)$ which depends on the value of the coupling. Higher is ϵ, higher will be the force which keeps the system near σ, and vice versa. The relation between the function $\Gamma(\epsilon)$ and the two-replica potential is very simple since they are one the Legendre transform of the other. Therefore one has

$$V_2(q_{12}) = \min_{\epsilon} \ (\Gamma(\epsilon) + \epsilon q_{12}) \qquad (2-\mathrm{A}.2)$$

with

$$\epsilon(q_{12}) = \frac{dV_2(q_{12})}{q_{12}} \ . \qquad (2-\mathrm{A}.3)$$

The two functions Γ and V_2 are conceptually different since they fix two different parameters, respectively ϵ and q_{12}. However the results they give are analogous if the parameters are opportunely chosen. This means that if one wants to obtain an equilibrium value of $q_{\sigma\tau}$ equal to q_{12} without imposing it as a constraint, one has to apply an external coupling ϵ equal to the one given in (2-A.3). For what concerns the minima of the two-replica potential this fact is clarifying. In the minima indeed the derivative of the potential is by definition null, and this implies that the force one has to apply to keep the system in these points is zero. This is nothing else than the definition of a local equilibrium, and corresponds to the free system stuck in one of its pure states.

Appendix 2-B

In this appendix the final form of the potential $V_2(q_{12})$ is explicitly calculated. The expression of $V_2(q_{12})$ in terms of the overlap matrix is

$$-\beta V_2(q_{12}) = \lim_{n,m\to 0} \frac{1}{2m} \left(\beta^2 \sum_{a,b} f(\mathbf{Q}_{ab}) + \log\det \mathbf{Q} \right) + \beta F_{free} \ . \qquad (2-\text{B}.1)$$

This expression has to be computed according to the particular form assumed for the overlap matrix. The first part is

$$\lim_{n,m\to 0} \frac{1}{m} \beta^2 \sum_{ab} f(\mathbf{Q}_{ab}) =$$

$$2\beta^2 f(q_{12}) + \beta^2 f(1) + \beta^2 (x_r - 1) f(r_1) - \beta^2 x_r f(r_0) \ . \qquad (2-\text{B}.2)$$

The second part is the most complicated one. It is useful to exploit the following relation:

$$\log\det \mathbf{Q} = \log\det\, Q^{11} + \log\det \left(Q^{22} - Q^{21} (Q^{11})^{-1} Q^{12} \right) \qquad (2-\text{B}.3)$$

where Q^{21} stands for $(Q^{12})^T$. With the chosen ansatz, from (2.7) and (2.8)

$$\log\det Q^{11} = 0 \qquad (2-\text{B}.4)$$

and

$$Q^{21} (Q^{11})^{-1} Q^{12} = q_{12}^2 \qquad (2-\text{B}.5)$$

is a constant matrix. In this way equation (2-B.3) becomes

$$\log\det \mathbf{Q} = \log\det R \qquad (2-\text{B}.6)$$

with

$$R_{ab} = Q^{22}_{ab} - q_{12}^2 = (1 - r_1)\ \delta_{ab} + (r_1 - r_0)\ \epsilon_{ab} + (r_0 - q_{12}^2) \ . \qquad (2-\text{B}.7)$$

To calculate the determinant of R one needs to solve the eigenvalue equation

$$(1 - r_1) v_a + (r_1 - r_0) \sum_b \epsilon_{ab} v_b + (r_0 - q_{12}^2) \sum_b v_b = \lambda v_a \ . \qquad (2-\text{B}.8)$$

Let me distinguish three cases:

i) If

$$\sum_b \epsilon_{ab} v_b = 0 \qquad \forall \quad a \qquad (2-\text{B}.9)$$

and, consequently,

$$\sum_b v_b = 0 \qquad (2-\text{B}.10)$$

one has

$$\lambda_1 = (1 - r_1) \ . \tag{2-B.11}$$

In (2-B.9) the number of independent equations is equal to the number of blocks, that is m/x_r; the degeneration of the previous eigenvalue is then

$$d_1 = m - m/x_r \ . \tag{2-B.12}$$

ii) If

$$\sum_b v_b = 0 \tag{2-B.13}$$

one obtains:

$$\lambda_2 = (1 - r_1) + x_r(r_1 - r_0) \tag{2-B.14}$$

because the elements of the vector $\mathbf{v}$ must be equal in blocks of size x_r. The number of equations determining λ_2 is one and thus one gets

$$d_2 = m - (m - m/x_r) - 1 = m/x_r - 1 \ . \tag{2-B.15}$$

iii) If the previous conditions are not satisfied, and the sums are all different from zero, equation (2-B.8) gives

$$\lambda_3 = (1 - r_1) + x_r(r_1 - r_0) + m(r_0 - q_{12}^2) \tag{2-B.16}$$

$$d_3 = 1 \ . \tag{2-B.17}$$

Expression (2-B.6) then becomes

$$\begin{aligned} \frac{1}{m}\log \det R = \log(1 - r_1) &+ \frac{1}{x_r}\log\left(1 + x_r\frac{r_1 - r_0}{1 - r_1}\right) \\ &+ \frac{1}{m}\log\left(1 + m\frac{r_0 - q_{12}^2}{1 - r_1 + x_r(r_1 - r_0)}\right) \xrightarrow[m\to 0]{} \\ \log(1 - r_1) &+ \frac{1}{x_r}\log\left(1 + x_r\frac{r_1 - r_0}{1 - r_1}\right) + \frac{r_0 - q_{12}^2}{1 - r_1 + x_r(r_1 - r_0)} \ . \end{aligned} \tag{2-B.18}$$

From (2-B.2) and (2-B.18) one obtains the final form

$$\begin{aligned} -2\beta V_2(q_{12}) = &\ 2\beta^2 f(q_{12}) + \beta^2(x_r - 1)f(r_1) - \beta^2 x_r f(r_0) \\ &+ \log(1 - r_1) + \frac{1}{x_r}\log\left(1 + x_r\frac{r_1 - r_0}{1 - r_1}\right) + \frac{r_0 - q_{12}^2}{1 - r_1 + x_r(r_1 - r_0)} \ . \end{aligned} \tag{2-B.19}$$

For the sake of completeness we note that there is a different method by which the potential can be computed, based on the formula

$$\begin{aligned} -\beta N V_2(q_{12}) = & \\ = \lim_{n\to 0}\lim_{R\to 1}\frac{1}{n}\frac{\partial}{\partial R} & \overline{\left(\int d\sigma \exp(-\beta H(\sigma))\left(\int d\tau \exp(-\beta H(\tau))\delta(q_{\sigma\tau} - q_{12})\right)^{R-1}\right)^n} \\ & - \overline{\log Z_{free}} \end{aligned} \tag{2-B.20}$$

where in the calculation of the average R has to be considered as an integer (compare with equation (2.4)). In this way the replicated partition function takes the form

$$Z^{n,R} = \overline{\int d\tau_a^r \exp\left[-\beta\left(\sum_{a=1}^{n}\sum_{r=1}^{R} H(\tau_a^r)\right)\right] \prod_{a=1}^{n}\prod_{r=2}^{R} \delta(\tau_a^1\tau_a^r - q_{12})} \qquad (2-\mathrm{B}.21)$$

where σ_a is set equal to τ_a^1. With this approach one obtains a $nR \times nR$ global overlap matrix $\mathbf{Q}$, formed by the $n \times n$ sub-matrices Q_{ab}^{rs} with $a, b = 1, \ldots, n;\ r, s = 1, \ldots, R$. In this way, the matrix Q^{11} encodes the overlap 1-1, the matrices Q^{1r} the overlap 1-2 and the matrices Q^{rs} with $r, s \neq 1$ encode the overlap 2-2. The ansatz that has to be taken for the various matrices is a mere translation into this context of the one given in Section 2.

The same line of reasoning can be applied in the computation of the three replica potential. Obviously, in both cases, the two methods are equivalent.

Chapter III: The three-replica potential

The three-replica potential is a natural generalization of the two-replica potential in which two configurations are kept fixed and a third system has to thermalize keeping given overlaps with them.

To proceed as in the case of the two-replica potential let us consider three independent real replicas of the system: The first replica (replica 1) freely thermalizes at a temperature T and one of its equilibrium configurations, ρ, is chosen and fixed. The second replica (replica 2) is constrained to thermalize at a given overlap q_{12} with ρ, then one of its constrained equilibrium configurations, σ, is chosen and fixed. Finally one computes the free energy of a third replica (replica 3) which is constrained to have an overlap q_{13} with ρ and an overlap q_{23} with σ.

The localization of the three replicas is then the following. Replica 1 is fixed in one of the equilibrium states of the free system. Replica 2 has thermalized in the manifold at overlap q_{12} with this state: if states of the free system are present in this manifold we can argue that replica 2 thermalizes catching their contribution so that the configuration σ will belong to one of them. In this case replica 2 is then in the proximity of a state at overlap q_{12} with replica 1 and the hope is that by varying q_{13} and q_{23} it is possible to induce replica 3 to thermalize in this state.

We can realize that the presence of the third replica is crucial: In the two-replica potential replica 2 gives non trivial information only when the value of q_{12} is sufficiently high to force it in the same equilibrium state of replica 1. In the three replica potential replica 3 plays the same role, but with respect to replica 2, which is now fixed at generic values of q_{12}. The advantage is that in this way one can analyze not the reference equilibrium state, but the other states present all around it.

As in the previous case, to have information on local or global equilibrium states of the free system one has to define the potential function and then look at its minima. The three-replica potential V_3 is defined in the usual way taking the difference between the constrained free energy of replica 3 and the free energy of the unconstrained system:

$$V_3(q_{12};q_{13}q_{23}) = F_{const}(q_{12};q_{13}q_{23}) - F_{free} \ . \tag{0.1}$$

The potential V_3 depends on all the three overlaps, but they have a different role: q_{12} represents the distance between the two fixed configurations and fixing it means to choose the region of the phase space we want to investigate; on the other hand q_{13} and q_{23} are the parameters by varying which, at fixed q_{12}, we can probe the landscape around the replica 1 and replica 2, looking for local equilibrium regions. Therefore in this case to reveal the presence of eventual states of the free system we must look at the minima of V_3 with respect to q_{13} and q_{23}, at fixed q_{12}.

1. The computation of the three-replica potential

The explicit expression of the three-replica potential is:

$$
\begin{aligned}
&-\beta N V_3(q_{12}|q_{13},q_{23}) = \\
&\overline{\log \int d\tau \exp(-\beta H(\tau))\ \delta(q_{\rho\tau}-q_{13})\ \delta(q_{\sigma\tau}-q_{23})} - \overline{\log Z_{free}}\ .
\end{aligned}
\tag{1.1}
$$

In equation (1.1) V_3 depends on the imposed constraints and on the fixed configurations. As in the case of V_2 we assume self-averageness with respect to the distributions of the two fixed configurations. For what concerns ρ this distribution is the usual Boltzmann measure, since replica 1 has thermalized freely. On the other hand replica 2 is itself a constrained system so that the distribution related to σ is the constrained measure

$$
\frac{1}{Z(\rho;q_{12})}\exp(-\beta H(\sigma))\ \delta(q_{\rho\sigma}-q_{12})
\tag{1.2}
$$

with

$$
Z(\rho;q_{12}) = \int d\sigma \exp(-\beta H(\sigma))\ \delta(q_{\rho\sigma}-q_{12})\ .
\tag{1.3}
$$

Expression (1.1) then becomes

$$
\begin{aligned}
&-\beta N V_3(q_{12}|q_{13},q_{23}) = \\
&= \overline{\frac{1}{Z_{free}}\int d\rho \exp(-\beta H(\rho)) \frac{1}{Z(\rho;q_{12})}\int d\sigma \exp(-\beta H(\sigma))\ \delta(q_{\rho\sigma}-q_{12}) \times} \\
&\overline{\log \int d\tau \exp(-\beta H(\tau))\ \delta(q_{\rho\tau}-q_{13})\ \delta(q_{\sigma\tau}-q_{23})} - \overline{\log Z_{free}}
\end{aligned}
\tag{1.4}
$$

where the integrations over ρ and σ represent the annealed averages over the fixed configurations and the integration on τ expresses the partition function of replica 3, of which we compute the free energy.

By the usual trick we get

$$
\begin{aligned}
&-\beta N V_3(q_{12}|q_{13},q_{23}) = \\
&= \lim_{n,m,l\to 0} \frac{1}{l} \overline{\log \int d\rho_a d\sigma_b d\tau_c \exp\left[-\beta\left(\sum_{a=1}^{n} H(\rho_a) + \sum_{b=1}^{m} H(\sigma_b) + \sum_{c=1}^{l} H(\tau_c)\right)\right] \times} \\
&\overline{\prod_{b=1}^{m} \delta(q_{\rho_1\sigma_b}-q_{12}) \prod_{c=1}^{l} \delta(q_{\rho_1\tau_c}-q_{13})\delta(q_{\sigma_1\tau_c}-q_{23})} - \overline{\log Z_{free}}\ .
\end{aligned}
\tag{1.5}
$$

Again we introduce the sub-matrices:

$$
\begin{aligned}
Q^{11}_{ab} &= q_{\rho_a\rho_b} \qquad a=1,\ldots,n;\ b=1,\ldots,n \\
Q^{12}_{ab} &= q_{\rho_a\sigma_b} \qquad a=1,\ldots,n;\ b=1,\ldots,m \\
Q^{22}_{ab} &= q_{\sigma_a\sigma_b} \qquad a=1,\ldots,m;\ b=1,\ldots,m \\
Q^{13}_{ab} &= q_{\rho_a\tau_b} \qquad a=1,\ldots,n;\ b=1,\ldots,l \\
Q^{23}_{ab} &= q_{\sigma_a\tau_b} \qquad a=1,\ldots,m;\ b=1,\ldots,l \\
Q^{33}_{ab} &= q_{\tau_a\tau_b} \qquad a=1,\ldots,l;\ b=1,\ldots,l
\end{aligned}
\tag{1.6}
$$

together with $Q^{21}_{ab} = Q^{12}_{ba}$, $Q^{31}_{ab} = Q^{13}_{ba}$, $Q^{32}_{ab} = Q^{23}_{ba}$, in such a way that the total overlap matrix $\mathbf{Q}$ is symmetric. In analogy with the case of V_2, the expression of V_3 in terms of $\mathbf{Q}$, after averaging over the disorder, is

$$-\beta V_3(q_{12}|q_{13}, q_{23}) = \operatorname*{Ext}_{\mathbf{Q}} \left\{ \lim_{n,m,l\to 0} \frac{1}{2l}\left(\beta^2 \sum_{a,b} f(\mathbf{Q}_{ab}) + \log\det\mathbf{Q}\right)\right\} + \beta F_{free} \ . \tag{1.7}$$

We have now to assume an ansatz for the various overlap sub-matrices. In doing this it is important to bear in mind the difference between the roles of the three real replicas. This difference is indeed encoded in the different form of the relative overlap matrices.

Q^{11} refers to the first free replica, while Q^{22} refers to replica 2, which thermalizes at *fixed* overlap q_{12} with 1. Both replicas are however independent from the third one, so that the form of Q^{11}, Q^{12} and Q^{22} is identical to the one assumed in the case of V_2 and the value of the variational parameters (x_r, r_1, r_0), which are functions of q_{12}, are determined by the same equations (2.11).

For what concerns Q^{33}, we have seen in the case of the two-replica potential that the effect of the constraint is to break the symmetry of the overlap matrix referred to the constrained system, therefore for Q^{33} is assumed a one step RSB ansatz with parameters (x_s, s_1, s_0):

$$Q^{33}_{ab} = (1-s_1)\delta_{ab} + (s_1 - s_0)\epsilon_{ab} + s_0 \ . \tag{1.8}$$

There is no reason to set $x_s = x_r$, since just as Q^{22} is broken independently from Q^{11}, the breakings of Q^{22} and Q^{33} have to be assumed independent; moreover, there are no algebraic motivations for this equality.

For what concerns Q^{13}, both the limit $\beta \to 0$ and the check of introducing a tentative additional parameter, show that it is correct to assume a form similar to Q^{12},

$$Q^{13}_{ab} = q_{13}\ \delta_{a,1} \ . \tag{1.9}$$

However, the same limit shows that this form is no longer valid for Q^{23}; namely, the first row will still be equal to q_{23}, but the rest of the matrix cannot be set equal to zero. Moreover, the structure of Q^{23} has to take into account the RSB form of Q^{22}: if replicas 2 are organized into clusters, it can be that the overlap of 3 with the particular cluster that contains the *first* replica σ_1 of 2 (this is the only replica of 2 *really* coupled to 3, as shown in (1.5)) is different from the overlap of 3 with any other cluster.

Therefore, we postulate a RSB form also for Q^{23}. This is possible if we break the symmetry in the rows of Q^{23} in the following way:

$$Q^{23}_{ab} = (q_{23} - w_{23})\delta_{a,1} + (w_{23} - z_{23})\epsilon_{a,1} + z_{23} \ . \tag{1.10}$$

In this expression $\epsilon_{a,1}$ is equal to one for $a = 1, \ldots, x$, where x is the breaking point, and zero elsewhere. We note that the second member of (1.10) does not depend on the index b since Q^{23} is broken into vertical rather than diagonal blocks and each row is made of constant elements. This one step RSB needs a breaking point x, but the genesis of the breaking shows clearly that for Q^{23} we must take x_r as the breaking point, that is the same as in Q^{22}.

In conclusion, the new variational parameters are:

$$x_s, s_1, s_0, w_{23}, z_{23} \ . \tag{1.11}$$

With these ansatz, the expression of V_3 is (see Appendix B for details)

$$\begin{aligned}
-2\beta V_3(q_{12}, q_{13}, q_{23}) = \underset{\substack{x_s, s_1, s_0 \\ w_{23}, z_{23}}}{\mathrm{Ext}} & \Big\{ 2\beta^2 f(q_{13}) + 2\beta^2 f(q_{23}) + 2\beta^2 (x_r - 1) f(w_{23}) \\
& - 2\beta^2 x_r f(z_{23}) + \ \beta^2 (x_s - 1) f(s_1) - \beta^2 x_s f(s_0) \\
& + \log(1 - s_1) + \frac{1}{x_s} \log\left(1 + x_s \frac{s_1 - s_0}{1 - s_1}\right) \\
& + \frac{s_0 - y}{1 - s_1 + x_s(s_1 - s_0)} \Big\}
\end{aligned} \tag{1.12}$$

with

$$\begin{aligned}
y = q_{13}^2 + & (q_{23} - w_{23})^2 (a + b + c) + 2(q_{23} - w_{23})(w_{23} - z_{23})(a + x_r(b + c)) \\
& + 2(q_{23} - w_{23})(z_{23} - q_{12}q_{13})(a + b x_r) + (w_{23} - z_{23})^2 x_r (a + x_r(b + c)) \\
& + 2(w_{23} - z_{23})(z_{23} - q_{12}q_{13}) x_r (a + b x_r)
\end{aligned} \tag{1.13}$$

and

$$\begin{aligned}
a &= \frac{1}{1 - r_1} \\
b &= -\frac{r_1 - r_0}{1 - r_1} \cdot \frac{1}{1 - r_1 + x_r(r_1 - r_0)} \\
c &= -\frac{r_0 - q_{12}^2}{(1 - r_1 + x_r(r_1 - r_0))^2} \ .
\end{aligned} \tag{1.14}$$

Expression (1.12) is very similar to the one of $V_2(q_{12})$ with (x_s, s_1, s_0) playing the role of (x_r, r_1, r_0) and y instead of q_{12}^2. Indeed, the saddle point equations for (x_s, s_1, s_0) are in form exactly identical to (2.11), changing q_{12}^2 into y. Moreover, V_3 has to be maximized with respect to w_{23} and z_{23}:

$$\begin{aligned}
(1 - x_r)\beta^2 f'(w_{23}) = (1 - x_r) & \ \frac{1}{1 - s_1 + x_s(s_1 - s_0)} [(q_{23} - w_{23})(b + c) \\
& + (w_{23} - z_{23})(a + x_r(b + c)) + (z_{23} - q_{12}q_{13})(a + b x_r)] \\
x_r \beta^2 f'(z_{23}) = x_r & \ \frac{1}{1 - s_1 + x_s(s_1 - s_0)} [(q_{23} - w_{23})c \\
& + x_r(w_{23} - z_{23})c + (z_{23} - q_{12}q_{13})(a + b x_r)] \ .
\end{aligned} \tag{1.15}$$

We note that the equations for (x_s, s_1, s_0) are coupled to equations (1.15) by means of y, that contains w_{23} and z_{23}.

Let us now examine under which conditions the case of V_2 is recovered. It turns out that

$$\begin{aligned}
V_3(q_{12} = 0, q_{13} = 0, q_{23}) &= V_2(q_{23}) \\
V_3(q_{12} = 0, q_{13}, q_{23} = 0) &= V_2(q_{13}) \ .
\end{aligned} \tag{1.16}$$

This is just what we expected for the following reason: Setting $q_{12}=0$ replica 2 is forced in the manifold orthogonal to replica 1. This manifold is a $N-1$-dimensional sphere which becomes identical to the whole phase space in the thermodynamic limit, therefore replica 2 thermalizes independently from replica 1, and is fixed in an equilibrium configuration. For the same reason, if we set, for example, $q_{13}=0$, also replica 3 will be in the manifold orthogonal to replica 1 and will thus behave independenlty of replica 1, the constraint 1-3 becomes, in this sense, harmless. However replica 3 is still subjected to the constraint q_{23}, thus the pair 2-3 reproduces the case of V_2. The same is true for $q_{23}=0$.

2. The shape of the three-replica potential

Our purpose is to study the potential V_3 with respect of q_{13} and q_{23} at various fixed values of q_{12}. In this way, through the position of replica 3, we can explore the neighborhood of replica 2, which in general is not a configuration of equilibrium for the free system. To this aim we have to look at the minima of the potential in the (q_{13}, q_{23}) plane, at fixed q_{12}. The equations of minimization of V_3 with respect of q_{13} and q_{23} are:

$$\begin{aligned}
\beta^2 f'(q_{13}) =& \frac{1}{1-s_1+x_s(s_1-s_0)}[q_{13}-q_{12}(q_{23}-w_{23})(a+bx_r) \\
&-q_{12}(w_{23}-z_{23})x_r(a+bx_r)] \\
\beta^2 f'(q_{23}) =& \frac{1}{1-s_1+x_s(s_1-s_0)}[(q_{23}-w_{23})(a+b+c) \\
&+(w_{23}-z_{23})(a+x_r(b+c))+(z_{23}-q_{12}q_{13})(a+bx_r)] \ .
\end{aligned} \tag{2.1}$$

The numerical analysis of equations (2.1) shows the following pattern:

i) For each value of q_{12} there is a solution of (2.1) with

$$\begin{aligned}
&q_{13}=q_{23}=0 \\
&V_3=0 \ .
\end{aligned} \tag{2.2}$$

This is the absolute minimum of the potential in the (q_{13}, q_{23}) plane and is analogous to the absolute minimum of the two-replica potential: it corresponds to the situation in which replica 3 sees a phase space identical to that of the unconstrained system and thermalizes catching the contribution of all the equilibrium states orthogonal to replica 1 and replica 2. We note that in this minimum the potential has to be zero for a very natural reason: replica 3 has to be sited somewhere in the phase space and this translates into the formula:

$$\int dq_{13}dq_{23}\ e^{-NV_3(q_{13},q_{23})}=1 \quad \forall q_{12} \ . \tag{2.3}$$

For $N\to\infty$ this implies that in the absolute minimum the potential must be zero, as it is in our case.

ii) For any value of q_{12} and for any temperature in the range (T_c, T_d), there is a minimum M_1 with

$$\begin{aligned} q_{13} &= q_{EA} \\ q_{23} &\sim q_{12} \end{aligned} \tag{2.4}$$

where q_{EA} is the self-overlap of the equilibrium state of replica 1. The interpretation of M_1 is very simple: the third replica is in the same pure state as the first one, and therefore their mutual overlap is equal to the self-overlap of the state to which they belong. This conclusion is confirmed by the fact that they have approximately the same distance with the second replica. Moreover if one looks at the overlap sub-matrix of replica 3 one finds that it is symmetric and with

$$s_0 = s_1 = q_{13} = q_{EA} \ . \tag{2.5}$$

M_1 has then exactly the same meaning as M for the two replica potential and reproduces the properties of the equilibrium state of replica 1. It is evident that these properties do not depend on the value of q_{12} since the state of replica 1 is fixed once for all independently of the other two replicas. Indeed the potential in M_1 remains constant with varying q_{12} and is equal to the two-replica potential evaluated in the secondary minimum:

$$V_3(M_1) = V_2(q_{EA}) \ . \tag{2.6}$$

What happens when q_{12} grows, is that also replica 2 approaches the state in which the first two are, until for $q_{12} = q_{EA}$ the three replicas are all in the same state and $q_{12} = q_{13} = q_{23} = q_{EA}$.

iii) More interesting is the presence of a minimum with the third replica close to the second one. For T in the usual range (T_c, T_d) and $0 \le q_{12} \le \bar{q}(T)$ we find a minimum M_2 with

$$\begin{aligned} q_{23} &\sim q_{EA} \\ q_{13} &\sim q_{12} \le \ q_{EA} \ . \end{aligned} \tag{2.7}$$

In M_2 q_{23} is very high, of the order of a self-overlap (see figure 3-1), this indicating that replica 3 is very close to replica 2. The presence of a minimum with these values of the overlaps means that there is a pure state near replica 2 and replica 3 has thermalized into it. Therefore we have found a state of the system at overlap $q_{13} \sim q_{12} \neq 0$ with the reference equilibrium state. This result confirms that a non trivial structure of the states indeed exists, and that finally, through the three-replica potential, one is able to reveal it. It is simple at this point to obtain the thermodynamical properties of the state corresponding to this minimum. In M_2 the phase-space accessible to replica 3 is just the phase-space relative to the pure state in which it has thermalized, therefore the free energy density f_3 of this state is given by

$$f_3 = F_{const}(M_2) = V_3(M_2) + F_{free} \tag{2.8}$$

On the other hand the self-overlap is as usual given by the overlap sub-matrix of replica 3, which is symmetric in M_2 as it must, and is thus identified with $s_1 = s_0$.

A serious check of the previous result consists in verifying whether the state corresponding to the minimum M_2 can be identified with a TAP solution, i.e. if its free energy and self-overlap satisfy the

TAP equations. This would be the final confirmation that a state of the free system has been found. The check can be done numerically and it turns out that in M_2 the relation holding between f_3 and s_1 is always the same as in the TAP approach. In other words, the state corresponding to M_2 actually coincides with that particular TAP solution specified by

$$\begin{aligned} f_{TAP} &= f_3 \\ q_{TAP} &= s_1 \ . \end{aligned} \tag{2.9}$$

Since in M_2 replica 2 and replica 3 are in the same state, one can expect that not only s_1 but also q_{23} is equal to the self-overlap q_{TAP} of the corresponding TAP solution. Actually, this is not true: q_{23} is very near to $s_1 = q_{TAP}$, but not exactly the same (the difference being of order 10^{-3}, see figure 3-1). The physical reason of this lies in the different role of the two replicas: replica 2 is quenched in the state corresponding to M_2 with a non equilibrium distribution, it is not in general a typical configuration of this state and then q_{23} is not a good measure of the self-overlap. On the other hand, replica 3 truly thermalizes into this state and thus s_1, which comes from matrix Q^{33}, identifies the correct self-overlap.

With varying q_{12} the minimum M_2 corresponds to different metastable states at different overlaps q_{13} with replica 1. These states will have therefore different free energies, energies and self-overlaps. In figures 3-1,3-2,3-3 it is shown the variation with q_{12} of some important quantities evaluated in M_2.

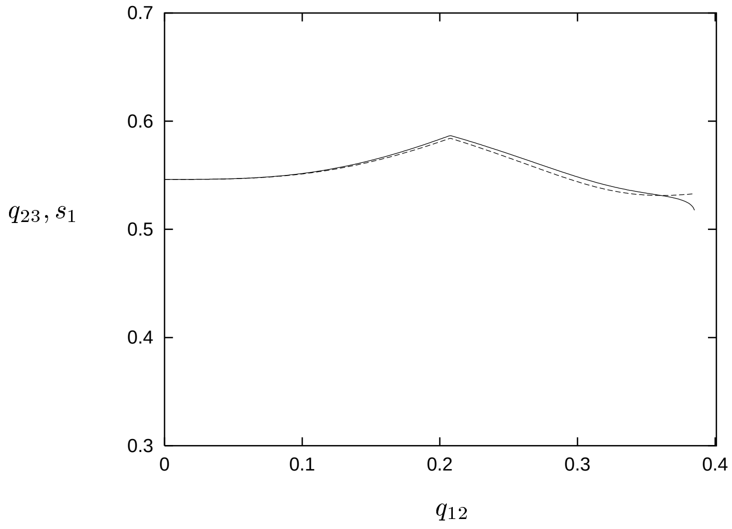

Figure 3-1: q_{23} and s_1 in M_2 as a function of q_{12} at β=1.64; q_{EA}=0.546, $\bar{q}$=0.385.

In figure 3-1 we can see the behaviour of q_{23} and s_1 in M_2. How I have already said, the value of q_{23}, even if different, remains however very close to the value of the self-overlap, given by s_1.

In figure 3-2 the potential $V_3(M_2)$ is reproduced, while in Figure 3-3 it is shown the behaviour of the energy difference $\Delta E = E_{const}(M_2) - E_{free}$.

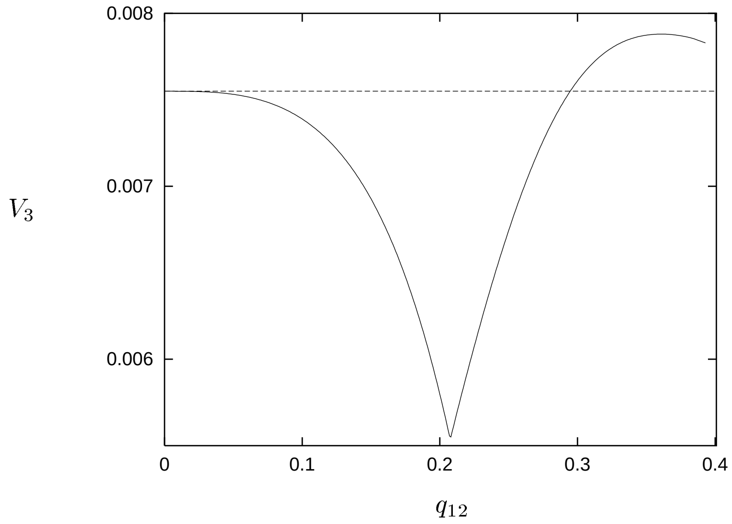

Figure 3-2: The potential V_3 in M_2 as a function of q_{12} at β=1.64; $q^\star$=0.295, $\bar{q}$=0.385.

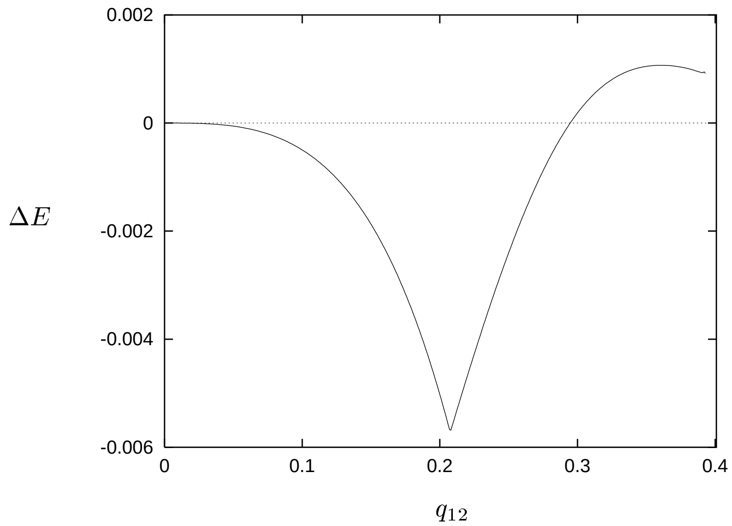

Figure 3-3: The energy difference ΔE in M_2 as a function of q_{12} at β=1.64; $q^\star$=0.295, $\bar{q}$=0.385.

Let us now examine and comment these curves.

For $q_{12} = 0$ we have $q_{13} = 0$, $q_{23} = q_{EA}$, $V_3(M_2) = V_2(q_{EA})$ and $\Delta E = 0$; this is trivial because we have seen that in this case V_3 reduces to $V_2(q_{23})$, which, evaluated in its secondary minimum, corresponds to an equilibrium state of the free system.

When $q_{12} \neq 0$ the second and the third replicas thermalize in a metastable state at overlap $q_{13} \sim q_{12}$

with replica 1. We can see that the energy and the free energy of this state decrease with decreasing the distance (i.e. increasing the overlap), until when $q = q_{rsb}$. At this point there is a cuspid in all the curves, and an inversion of the previous behaviour takes place: the energy and free energy of the metastable state corresponding to M_2 starts increasing. We note that the value q_{rsb} is exactly the same as the one found in the two replica potential. This point therefore corresponds to the value of q_{12} at which the sub-matrix Q_{22} encounters a replica symmetry breaking and passes from an RS form to a 1-step RSB one. Moreover, since the sub-matrix Q_{23} has the same structure as Q_{22}, it also becomes RSB in this point. From a technical point of view it is then clear that the cuspid is related to a change of solutions of the saddle point equations. The physical interpretation of this replica symmetry breaking is the one exposed in the previous chapter, however we will return on this argument in the next chapter for a more complete explanation.

Increasing more q_{12} there is a value $q^\star$ for which

$$\Delta E(q^\star) = 0 \; . \tag{2.10}$$

The fact that in this point the energy is equal to that of the unconstrained system means that replicas 2 and 3 are in a state of the same kind as the one chosen by the unconstrained system, that is one of the equilibrium states of the free system. This situation is analogous to the what happens in the minimum M of V_2, and indeed we have

$$\begin{aligned} &s_1(q^\star) = q_{EA} \\ &V_3(q^\star) = T\Sigma = V_2(q_{EA}) \; . \end{aligned} \tag{2.11}$$

For $q_{12} = q_{max}$ there is a maximum and the behaviour of the energy and the potential changes, decreasing again.

Finally, at $q_{12} = \bar{q}$ the curves end: this means that the closest metastable state to replica 1 is at overlap $\bar{q}$ with it, and that for $q_{12} > \bar{q}$ no more states are found around the reference state. The value of $\bar{q}$ is always less or equal to the value of the self-overlap of the reference state, this indicating that the metastable state found at $\bar{q}$ is well separated with respect of the equilibrium state of replica 1.

Resuming, we have the following picture: at temperature T with $T_c < T < T_d$, there is an exponentially high number of equilibrium states partitioning the phase space and the first unconstrained replica will thermalize into one of them. Through the potential V_3 we are able to see many other states at various distances from the it. For $q_{12} < \bar{q}$ we have a continuous spectrum of possible overlaps, each of them corresponding to a *different* kind of state, whose energy is either higher, equal or lower than the equilibrium one. From our discussion follows that the closest states of the same kind and with the same equilibrium energy as the reference one, are found at overlap $q^\star$ with it. At smaller distances there are local equilibrium states with higher energy, the closest of which are found at overlap $\bar{q}$.

3. Temperature dependence

Up to this moment we have studied V_3 at fixed temperature; now we examine the evolution of the system with T, in particular in the two limits $T \to T_s$ and $T \to T_d$.

First of all, we remind that choosing a particular temperature implies to select a particular class of equilibrium states. This means that at different temperatures replica 1 is sited in a different kind of state, corresponding to a different class of TAP solutions. In this way at different temperatures the potential V_3 explore the phase space with respect to different reference states.

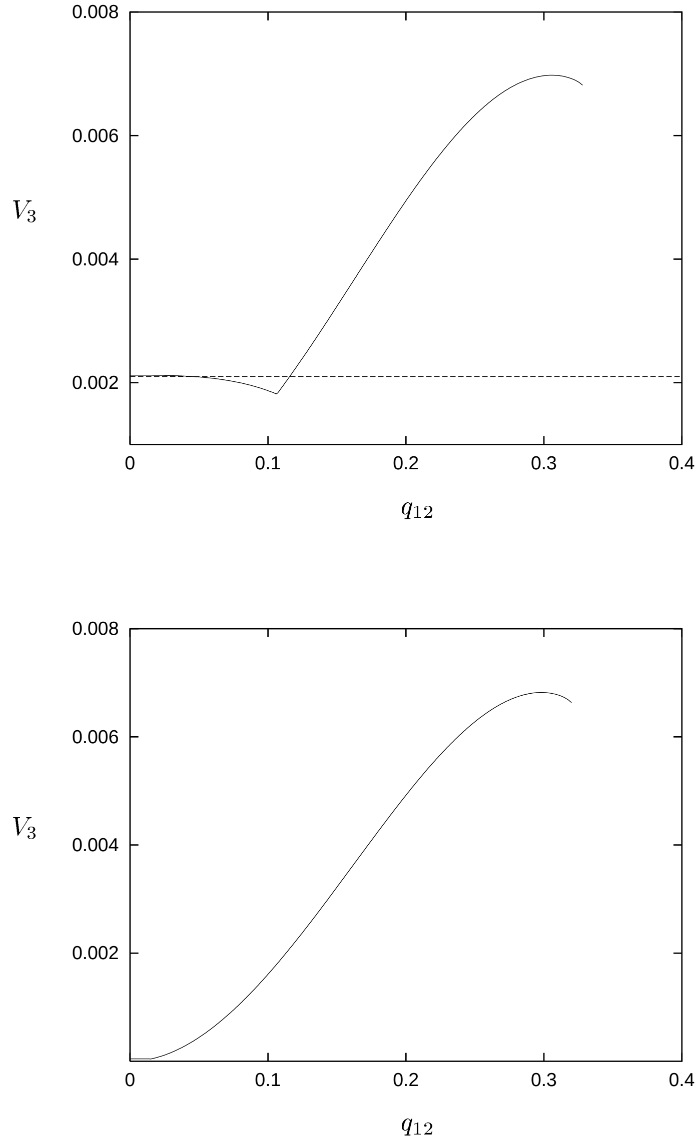

Figure 3-4 a,b: The potential V_3 in M_2 as a function of q_{12} at β=1.69 (figure a) and at β=β_s=1.706 (figure b).

From what said above, the behaviour of the minimum M_1 is modified with varying T just in a trivial way: M_1 indeed corresponds to replica 3 in the same state as replica 1, and this state is different at different temperatures.

Let us now look at M_2.

With decreasing T the equilibrium state of replica 1 has lower free energy. It is then reasonable that the range of q_{12} in which the potential is negative restricts, since the states with free energy lower than the equilibrium one are globally less (see the TAP spectrum of figure 1-1). This is what actually happens, as shown in figure 3-4: we can see also that at T_s, when the reference state has the lowest possible free energy and all the states around it must have greater free energy, the potential V_3 is always positive.

At T_s the configurational entropy Σ of the dominant equilibrium states goes to zero [21,26]; this means that the number of these states becomes finite and they *all* have zero overlap with each other. In this situation one expects that, given an equilibrium state, the closest equilibrium one is at overlap zero with it; indeed one can see in figure 3-4 that $q^\star \to 0$ when $T \to T_s$.

What happens at T_d is more interesting. First, we know that at this temperature the equilibrium states have the highest energy density, so we expect not to find local equilibrium states at higher energy; this is exactly what we have, since $\bar{q} \to q^\star$ for $T \to T_d$. Moreover, at this temperature Σ reaches a finite value, meaning that the number of the equilibrium states is still exponentially high; therefore, it is not clear *a priori* what is their minimum mutual distance. The very interesting feature shown by our potential is that

$$\bar{q}, q^\star \to q_d \quad \text{for} \quad T \to T_d \tag{3.1}$$

where q_d is the value of q_{EA} at the dynamical transition.

Thus at T_d the overlap between the reference threshold equilibrium state and its nearest equilibrium state becomes equal to their self-overlap and the two states are merged together. This indicates that at T_d threshold states are continuously proximate one to the other, even if it is not clear if this is a feature of the dynamical transition, or a characteristic of the threshold states at each temperature. In each case, what equation (3.1) says is that as T approaches T_d, the closest equilibrium states collapse into a single state of self-overlap q_d. One can also examine how this collapse takes place, and discover that it follows a power law with respect to the temperature. For example, for $T \sim T_d$ and $p=3$ one finds that

$$\begin{aligned} q_{EA} &= (T_d - T)^{1/2} + q_d \quad , \quad q_d = 0.5 \\ q^\star &= a\ (T_d - T)^b + c\ . \end{aligned} \tag{3.2}$$

A fit of the numerical data gives

$$\begin{aligned} a &= -1.2 \\ b &= 0.24 \\ c &= 0.5004\ . \end{aligned} \tag{3.3}$$

As we have seen, this indicates that $q^\star$ reaches q_d at T_d. The value of the exponent b can be less firmly established; indeed, if one makes a fit fixing $c = 0.5$ one gets

$$b = 0.30\ . \tag{3.4}$$

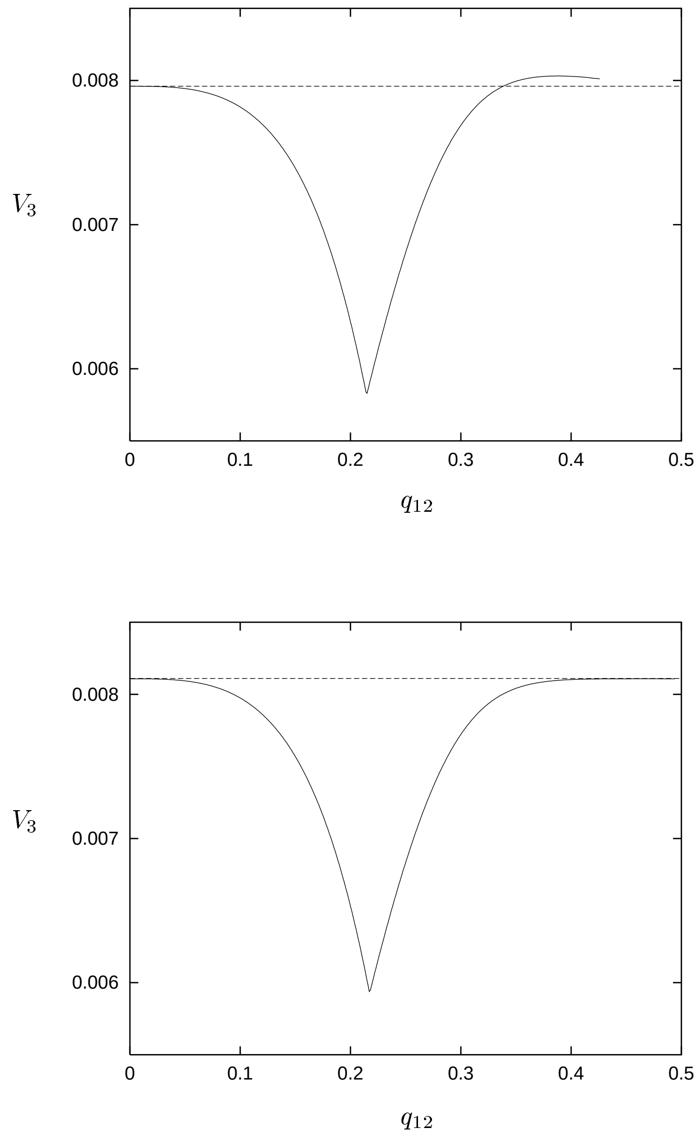

Figure 3-5 a,b: The potential V_3 in M_2 as a function of q_{12} at β=1.635 (figure a) and at β=β_d=1.633 (figure b).

This behaviour of the threshold states has another surprising consequence: it indicates that the equilibrium states are not uniformly distributed in the phase-space, which would actually be the simplest possibility. Indeed, if one hypothesizes a uniform distribution on the sphere, the volume available to each equilibrium state multiplied by the total number of the states must give the total volume of the sphere. This fact implies a simple relation between the number of equilibrium states and their minimum mutual overlap q:

$$\ln\left(1-\frac{q^2}{q_{EA}^2(T)}\right)=-2\Sigma(T)\ . \tag{3.5}$$

From (3.5) we deduce that q should remain definitively different from q_d when $T\to T_d$, since $\Sigma(T_d)$ has a finite value. But, as we have seen, this does not happen, and therefore the hypothesis of the random distribution has to be discarded.

Finally, one can study the potential for $T > T_d$. In this range the dominant equilibrium state is the paramagnetic one and the two replica potential has just the minimum in zero; for this reason the minimum M_1 of V_3 disappears, and no other minima with $\Delta E = 0$ exist. However we still find the minimum M_2 in a restricted range of q_{12} (see figure 3-6), to point out the existence of local equilibrium states even at temperature greater than T_d, corresponding to TAP solutions surviving above T_d.

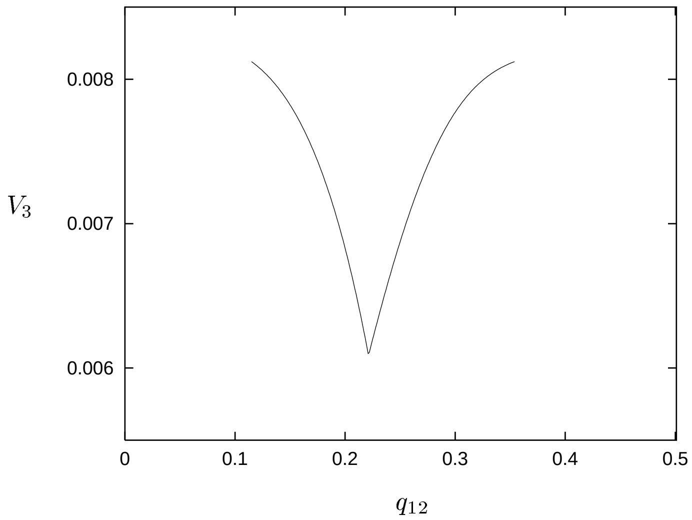

Figure 3-6: The potential V_3 in M_2 as a function of q_{12} at $\beta_{last}<\beta=1.635<\beta_d$.

This situation holds up to a temperature $T_{last} > T_d$ over which all non trivial minima disappear. For $p = 3$ we have

$$\begin{aligned} \beta_c &= 1.706 \\ \beta_d &= 1.633 \\ \beta_{last} &= 1.573 \ . \end{aligned} \tag{3.6}$$

This result is a confirmation of the existence of metastable pure states also in the temperature range in which the statics is dominated by the paramagnetic state. It remains probably counterintuitive in that the paramagnetic state is usually associated to a situation in which the system is ergodic, as it actually happens in the high temperature range $T > T_{TAP}$. This is however also what the TAP approach provides for and has been shown to be true with dynamical methods (with regard to this see [41]).

4. A comparison with a dynamical approach

In Chapter II we briefly described a dynamical analysis complementare to the statical one, which confirms the results found with the two-replica potential. Similarly, also in the case of the three-replica potential a parallel dynamical approach can be performed [42].

This time the initial configuration of the evolving system is chosen with the following strategy. A first configuration ρ is extracted with the Boltzmann measure and fixed as reference point, then another configuration σ at overlap q_{12} with the first one is extracted using the constrained distribution (1.2): this second configuration is considered as the starting point of the evolving system. The first configuration has the same role as replica 1 in the three-replica potential and lies in an equilibrium state. The initial configuration is chosen as replica 2 was, and if metastable states are present at overlap q_{12} with replica 1, it will belong to one of these states. The configuration $\sigma(t)$ of the evolving system is the dynamical analogous of replica 3, and we can expect it to evolve according to the statical scenario outlined with the three-replica potential.

We know from the previous sections that for $q_{12} < \bar{q}$ there are metastable states around the equilibrium state M_1 of replica 1, and replica 2 is actually in one of them, M_2. Since our system starts its evolution exactly where replica 2 is fixed, we expect it to relax properly in the metastable state identified by M_2. On the other hand it is not clear what happens when $q_{12} > \bar{q}$. In this case replica 2 is not fixed in any state and the three-replica potential ceases to form the minimum M_2. One can guess that the initial configuration is enough close to replica 1 to let the system relax into the equilibrium state M_1. However the value of $\bar{q}$ is usually not too big so that this hypothesis may not be always true.

To check all these questions we must, as usual, solve the equations for the dynamical quantities. In this case, besides the standard correlation function $C(t,t') = \overline{<\sigma(t)\cdot\sigma(t')>}$, we have the correlation function $C(t,0) = \overline{<\sigma(t)\cdot\sigma>}$ which measures how much the system is far from the initial configuration , and the correlation function $Q(t) = \overline{<\sigma(t)\cdot\rho>}$ which measures the distance from the first fixed configuration. We note that also in the dynamical computation replicas must be introduced to exploit the averages over the distributions of the fixed configurations. In this way the correlation functions that we have defined are actually replicated to generate a sort of dynamical correlation matrices analogous to the overlap submatrices (1.6):

$$\begin{aligned} C(t,t') &= \overline{<\sigma(t)\cdot\sigma(t')>} \to Q_{33} \\ C_a(t) &= \overline{<\sigma(t)\cdot\sigma_a>} \to Q_{23} \\ Q_a(t) &= \overline{<\sigma(t)\cdot\rho_a>} \to Q_{13}\ . \end{aligned} \tag{4.1}$$

The similarity with the three-replica potential suggests to assume for the correlation matrices (4.1) the same ansatz assumed for the overlap matrices (1.6). At this point the equations for the dynamical quantities can be solved in the limit $t,t'\to\infty$ [42]. What is found is that the asymptotic dynamics of the system is of equilibrium, i.e. time-translation invariance and the fluctuation-dissipation relation hold, moreover the equations for the asymptotics values of the dynamical correlation matrices are exactly the same as the minima equations for the overlap matrices in the three-replica potential (that is equations (1.15) and (2.1)).

We know that for $q_{12} < \bar{q}$ the potential V_3 has two non trivial minima, M_1 and M_2, however the dynamical equations admit a unique solution for any finite time and therefore only one of these two minima can be reached dynamically. Integrating numerically the dynamical equations one finds that when $q_{12} < \bar{q}$ the system rapidly relaxes in the metastable state corresponding to M_2, this confirming our expectations. On the other hand for $q_{12} > \bar{q}$ the system always relaxes in the equilibrium state of replica 1, with a timescale which increases at decreasing overlaps and diverges at $\bar{q}$. For high values of q_{12} this is indeed the most reasonable behaviour since the system starts its evolution very close to replica 1. More interesting is that the same thing actually happens also for values not too big of q_{12}, up to the value given by $\bar{q}$: in this sense $\bar{q}$ must be considered as the basin of attraction of a typical equilibrium state.

5. Conclusions

In this chapter we have seen how the three-replica potential is able to provide important information on the structure of the states in the p-spin sperical model.

The most important results obtained with this method concern the disposition of metastable states around a typical equilibrium state. Given a reference equilibrium state we find that

- There are local equilibrium states with overlap different from zero with it.
- The nearest state is found at overlap $\bar{q}(T)$ with it.
- The nearest equilibrium state is found at overlap $q^\star(T)$ with it.
- The nearest states have free energy density greater than the equilibrium one.
- At T_d threshold states are infinitely proximate one to the other.
- At T_d the equilibrium states are not uniformly distributed in the phase space.

Appendix 3-A

In this appendix the final form of the potential V_3 is calculated. We have:

$$-\beta V_3(q_{12},q_{13},q_{23}) = \lim_{n,m,l\to 0} \frac{1}{2l}\left(\beta^2 \sum_{a,b} f(\mathbf{Q}_{ab}) + \log\det\mathbf{Q}\right) + \beta F_{free} \ . \qquad (3-\mathrm{A}.1)$$

The first part is

$$\begin{aligned}\lim_{n,m,l\to 0} \frac{1}{l}\beta^2 \sum_{ab} f(\mathbf{Q}_{ab}) =& 2\beta^2 f(q_{13}) + 2\beta^2 f(q_{23}) + 2\beta^2(x_r-1)f(w_{23}) \\ & -2\beta^2 x_r f(z_{23}) + \beta^2 f(1) + \beta^2(x_s-1)f(s_1) - \beta^2 x_s f(s_0) \ .\end{aligned} \qquad (3-\mathrm{A}.2)$$

For the second part we use the following relation:

$$\begin{aligned}&\log\det\mathbf{Q} = \\ &= \log\det Q^{11} \\ &+ \log\det[Q^{22} - Q^{21}(Q^{11})^{-1}Q^{12}] \\ &+ \log\det[Q^{33} - Q^{31}(Q^{11})^{-1}Q^{13} \\ &\quad - (Q^{23} - Q^{21}(Q^{11})^{-1}Q^{13})^T(Q^{22} - Q^{21}(Q^{11})^{-1}Q^{12})^{-1}(Q^{23} - Q^{21}(Q^{11})^{-1}Q^{13})]\end{aligned} \qquad (3-\mathrm{A}.3)$$

where the previous notation for the transposed matrices is adopted. The first two parts in the r.h.s reproduce the case of the two replicas potential and both go to zero when $(n,m,l)\to 0$.

The remaining parts of the determinant are:

$$\begin{aligned}Q^{31}(Q^{11})^{-1}Q^{13} &= q_{13}^2 \\ Q^{21}(Q^{11})^{-1}Q^{13} &= q_{12}q_{13} \\ Q^{21}(Q^{11})^{-1}Q^{12} &= q_{12}^2\end{aligned} \qquad (3-\mathrm{A}.4)$$

constant matrices. Finally, let us compute the inverse of $A = Q^{22} - q_{12}^2$:

$$A_{ab} = (1-r_1)\delta_{ab} + (r_1 - r_0)\epsilon_{ab} + (r_0 - q_{12}^2) \ , \qquad (3-\mathrm{A}.5)$$

that is,

$$(A^{-1})_{ab} = \frac{1}{1-r_1}\,\delta_{ab} + \frac{r_0-r_1}{1-r_1}\cdot\frac{1}{1-r_1+x_r(r_1-r_0)}\,\epsilon_{ab} + \frac{q_{12}^2 - r_0}{(1-r_1+x_r(r_1-r_0))^2} \ . \qquad (3-\mathrm{A}.6)$$

Now it is possible to calculate the product

$$\pi = (Q^{23} - Q^{21}(Q^{11})^{-1}Q^{13})^T(Q^{22} - Q^{21}(Q^{11})^{-1}Q^{12})^{-1}(Q^{23} - Q^{21}(Q^{11})^{-1}Q^{13}) \ . \qquad (3-\mathrm{A}.7)$$

As can be easily seen the three matrices have the correct form, since they are RSB matrices with the same breaking point x_r. Due to this fact, the result of this product is a constant, although very complicate, given in equation (1.13).

Now it remains to calculate:

$$\log\det[Q^{33}-y] \tag{3-A.8}$$

proceeding as in Appendix A, with y instead of q_{12}^2, we get

$$\frac{1}{l}\log\det[Q^{33}-y]=\log(1-s_1)+\frac{1}{x_s}\log\left(1+x_s\frac{s_1-s_0}{1-s_1}\right)+\frac{s_0-y}{1-s_1+x_s(s_1-s_0)}\;. \tag{3-A.9}$$

In this way we recover equation (3-A.9).

Chapter IV: A comparison with the constrained complexity

The three-replica potential gives an important confirmation of the existence of a non trivial structure of the states: it shows that there are local and global equilibrium states at non zero overlap with an equilibrium reference one, and indicates that the distribution of the states in the phase space is not uniform. Therefore, of the two possible scenarios outlined at the end of Chapter I, the second is actually the right one.

In this context one has to persist in looking for non standard methods in order to analyze the hidden structure revealed by the three-replica potential. An interesting tool would be a quantity in some sense analogous to the $P(q)$, able to give the same kind of information, but also to catch all those states that the usual overlap distribution of the replica method does not see. Bearing in mind the reason for which the standard $P(q)$ is trivial, that is the presence of a huge number of states each one with a vanishing weight, one can then think at an alternative distribution quantity which avoids this problem. This can be done within the TAP approach, as we will show in this chapter, basically disregarding the thermodynamical weights of the states and performing a purely entropical computation.

1. The constrained complexity

In the TAP approach, as we have already seen, the exponentially high number of solutions is organized into different classes, each class corresponding to a different value of the zero-temperature energy density E. It is possible in a standard way to compute the complexity $\Sigma(E)$ of each class [26]:

$$\Sigma(E) = \stackrel{\mathrm{def}}{=} \lim_{N\to\infty} \frac{1}{N} \overline{\log \mathcal{N}(E)} \ . \tag{1.1}$$

that is the logarithm of the number of solutions with energy density E. This complexity can also be computed within the replica method through the two-replica potential, and is given by the value of the potential function in the secondary minimum.

The concept of complexity can be generalized to introduce an overlap dependent quantity: one fixes a reference TAP solution of energy E_1, and simply counts how many TAP solutions of energy E_2 are present at overlap q with the reference solution. The logarithm of this number is defined to be the *constrained complexity*:

$$\Sigma_c(E_2, q|E_1) \stackrel{\mathrm{def}}{=} \lim_{N\to\infty} \frac{1}{N} \overline{\log \mathcal{N}(E_2, q|E_1)} \ . \tag{1.2}$$

The strategy of this definition resembles the one of the potential function. However we are here within the TAP approach so that the computation of the complexity (1.2) is conceptually very different from the one of the potential. From a technical point of view one has to handle directly with mean field equations for averaged quantities and not with Boltzmann or constrained measures in the configurations space. Physically what one computes is here an entropy, while in the potential method one substantially has a free energy.

We will not enter in the details of the computation of Σ_c, but just say that it is performed integrating over all the TAP solutions which satisfy the imposed requirements (see [27,28]). What one finally obtains is a function which depends on three variables, the energy of the fixed solution E_1, the energy of the counted solutions E_2, and the overlap q at which one is counting. At this point we can analyze the behaviour of Σ_c with respect to each one of its variables, depending on what we are most interested in. Since the present aim is to compare the results given by this method with the ones obtained with the three-replica potential we will fix in the following the reference TAP solution to be an equilibrium one: to do this we choose $E_1 = E_{eq}(\beta)$, where $E_{eq}(\beta)$ is the zero-temperature energy density of the dominant TAP solutions at temperature β. In this way Σ_c counts how many states of energy density E_2 are present at distance q from a fixed equilibrium state.

2. The results

The main result we can gain with the constrained complexity is probably the information it gives on the the overlap spectrum. To extract this information we fix also the energy E_2 of the counted solutions and analyze the dependence of Σ_c with respect to the overlap q.

We can have an intuitive idea on what the behaviour of the constrained complexity should be. First of all, from the computation of the standard $P(q)$ we know that the most probable value for the overlap is $q = 0$, thus the most part of solutions, in the thermodynamic limit all, must be at zero overlap with the reference one. Therefore Σ_c must have its maximum for $q = 0$ and be equal in this point to the global standard complexity, that is $\Sigma_c(E_2, 0|E_1) = \Sigma(E_2)$. In second place, we can expect that, with increasing q, Σ_c decreases, since this corresponds to consider smaller and smaller portions of the phase space into which looking for TAP solutions of energy E_2. Finally, when q is too high, we can expect not to find anymore solutions in an exponential number, and thus at a certain point Σ_c has to become zero.

In figure 4-1 Σ_c is plotted as a function of the overlap. We can see that the intuitive idea is actually reproduced. However this curve provides also some absolutely not trivial information. First of all, it is a continuous curve: this indicates that there are states of energy E_2 in an exponentially high number, at each value of the overlap starting from zero up to a last value q_{last}. For $q > q_{last}$ Σ_c becomes negative this meaning that there are no more solutions of energy E_2. Thus q_{last} represents the overlap with the reference solution of the nearest solutions of energy E_2.

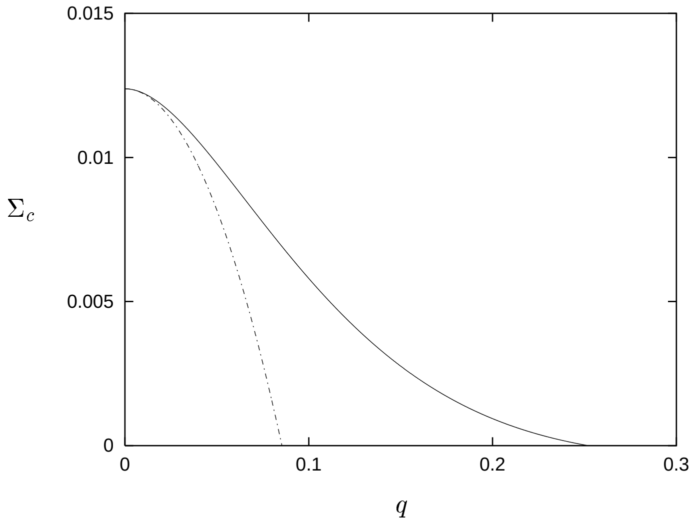

Figure 4-1: The constrained complexity Σ_c as a function of the overlap q (full line), with $E_1{=}E_2{=}E_{eq}{=}{-}1.156$, for $\beta{=}1.64$ and $p{=}3$. The self overlap of the two states is $q_1{=}q_2{=}0.55$, while $\Sigma_c{=}0$ at $q_{last}{=}0.25$. The dashed-dotted line is the curve predicted by a random distribution of the states (see the text). For $q{=}0$ both the curves coincide with the unconstrained complexity $\Sigma(E_2)$.

Varying E_2 we obtain curves very similar to the one of figure 4-1, with the value of q_{last} increasing with increasing the energy. However the value of q_{last} always remains different from the self-overlap of the states, this indicating that the nearest solutions are well separated from the reference one. An analogous result was found in the potential method.

When the value of E_2 is just below the threshold ($E \in [E_{th} - 5 \times 10^{-4}, E_{th}]$), Σ_c presents an anomalous behaviour: the intuitive decreasing behaviour, of clear geometric origins, still remains up to a high value of q, where Σ_c starts increasing and develops a small maximum. This indicates a sort of clustering of states with high energy at small distances, and is surely a very interesting result.

The three-replica potential is able to find states of the system at non zero overlap with the reference equilibrium one. However at each value of the overlap just one individual state is seen, the one in which replica 3 thermalizes. The process of thermalization of replica 3 is not something that one can control: once fixed the imposed overlaps it equilibrates following a constrained measure which automatically select a state. Nothing therefore is said about all the other states eventually present at the same distance with replica 1. On the other hand with the present method one can freely choose the value of E_2 and focus on different kinds of states to look for at a certain distance with the fixed one. The new result is that many kinds of states are present at various overlaps with the reference one, and, more than this, these states are exponentially numerous.

The three-replica potential gives an indication on the distribution of the states in the phase space, indeed from (3.5) we can deduce that the equilibrium states are not uniformly distributed in the phase space It is possible to analyze this problem also within this approach. If we assume a uniform distribution it is simple to obtain the consequent constrained complexity: in this case, the number of states at distance q from a given fixed point in the phase space is simply given by the total number of states multiplied by the volume of the manifold defined by fixing q. The resulting curve is plotted together with the real constrained complexity in figure 4-1. The two curves are definitely different, and this actually happens whatever is the chosen value of E_2. Therefore we can say that *all* the states, and not only the equilibrium ones, are not uniformly distributed. We can also see that the violation of the uniform distribution is in the direction of having a higher number of states when looking at smaller distances.

The three-replica potential gives an interesting information on the structure of the threshold states: what it turns out is that these states at the dynamical transition are continuously connected one with respect to the other. To check this point with the constrained complexity we must to set $E_1 = E_2 = E_{th}$, that is we fix a threshold state and counts how many other threshold states are present at overlap q with it. The obtained curve is qualitatively similar to the one of figure 4-1, but with a very important difference. Indeed in this case what happens is that

$$\Sigma_c(q) \to 0 \quad \text{for} \quad q \to q_{th}(\beta) \tag{2.1}$$

where $q_{th}(\beta)$ is the self overlap of the threshold states at the temperature β we are considering. This result says that, fixed a threshold state, other threshold states with vanishing complexity are found until a distance zero from the fixed one. This confirms what the three-replica potential provides for. Moreover in this context we can also see that this property of the threshold states is independent of the temperature, and thus truly concerns their geometrical structure, not being an exclusive feature of the dynamical transition.

3. How to reproduce the three-replica potential

In this section we will show how it is possible to approximately obtain the curve of the three-replica potential in the non trivial minimum, starting from the constrained complexity. This will once again confirm that the two general approaches, the replica approach and the TAP approach, actually provides with the same results, and are mutually consistent.

In the case of a free system, the replica approach gives directly the global free energy density F_{free} of the system. As we have seen in the first chapter we can obtain F also in the TAP approach. To this end we must look for the dominant among all TAP solutions, minimizing the generalized free energy $\phi = f - T\Sigma(f)$. The value of ϕ in its minimum gives precisely the free energy F_{free}.

In the case of a constrained system we can in the same way express the quantities obtained with the replica method in terms of properties of TAP solutions. We can for example consider the situation of the two-replica potential, in which replica 2 is constrained to thermalize at overlap q_{12} with a reference equilibrium state. In this case the system can only access to the states present at overlap q_{12}, and the two-replica potential then gives the global free energy related to the dominant among these states. In terms of TAP solutions we can say that the system tries to minimize the generalized free energy $\phi_c(f, q_{12}) = f - T\Sigma_c(f, q_{12})$, where $\Sigma_c(f, q)$ is the complexity of the solutions of free energy f present at overlap q_{12} with replica 1. The value of this function $\phi_c(f, q_{12})$ in its minimum $\bar{f}$ gives the global free energy of the constrained system, and thus $\phi_c(\bar{f}, q_{12}) - F_{free}$ gives the two-replica potential. In the situation of the three-replica potential, replica 2 is fixed in one of the dominant states at overlap q_{12}. This state corresponds to a TAP solution with individual free energy given by the value $\bar{f}$ which minimizes the function $\phi_c(f, q_{12})$. In the minimum M_2 replica 3 thermalizes in the same state of replica 2, and the potential $V_3(M_2)$ is therefore given by $\bar{f}$ minus F_{free}.

The interesting point is that we now have the complexity $\Sigma_c(f, q_{12})$: we have simply to consider the constrained complexity introduced in this chapter, set $E_1 = E_{eq}$, and express it as a function of the free energy density f of the counted solutions. Therefore we can compute the function $\phi_c(f, q_{12})$, minimize it, and obtain the values $\bar{f}$ and $\phi_c(\bar{f}, q_{12})$.

In figure 4-2 and 4-3 are shown the curves $\Sigma_c(f, q_{12})$ as function of f at various values of the overlap. The first figure is relative to the normal behaviour of Σ_c: for $q_{12} = 0$ we have the usual unconstrained complexity, then at increasing overlaps the curves gets lower and lower, according to what seen in the previous sections.

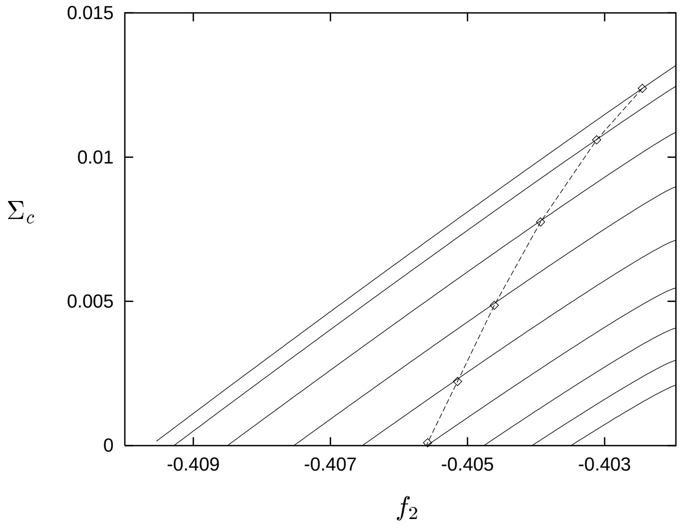

Figure 4-2: The constrained complexity Σ_c as a function of the free energy $f_2=f(E_2,\beta)$, at various values of the overlap q and $E_1=E_{eq}=-1.156$, for $\beta=1.64$ and $p=3$. The first curve on the top has $q=0$ and thus corresponds to the unconstrained complexity $\Sigma(f_2)$. The squares indicate the minimum of the function ϕ_c (see Section 4), which reaches the axis $\Sigma_c=0$ at $q_{low}=0.113$.

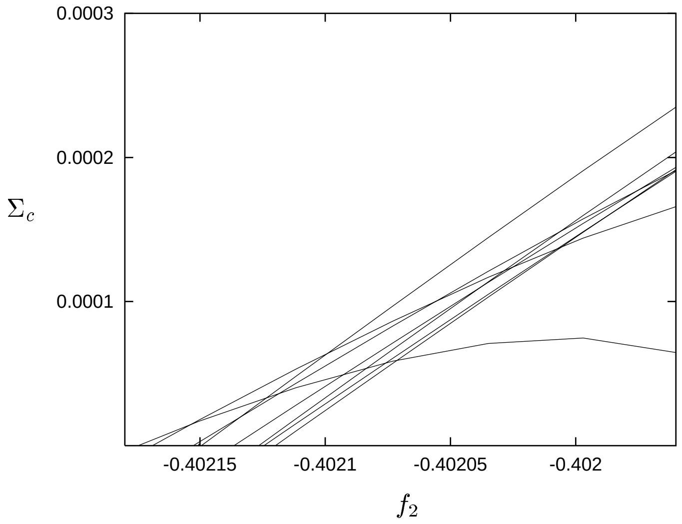

Figure 4-3: The constrained complexity Σ_c as a function of the energy $f_2 = f(E_2, \beta)$ just below the threshold, at various values of q. The value q_{max} corresponds to the curve whose intersection with the axis $\Sigma_c = 0$ starts going to the left with increasing q.

The second figure corresponds to the anomalous behaviour found in a narrow range of free energies just below the threshold. We can see that the curves continue to globally decrease with q_{12} until a value q_{max} of the overlap, then they begin to reverse, folding upwards. The value q_{max} corresponds to the curve whose intersection with the $\Sigma_c = 0$ axis starts going backward to the left with increasing q_{12}. This behaviour, when examined at a fixed value of the energy, provides for a maximum at high values of the overlap, how said in the previous section.

In figure 4-2 for each value of q_{12} it is signed on the corresponding curve the point that minimizes ϕ_c. We can see that there is a value q_{low} at which the minimum of ϕ_c reaches the axis. For higher values of the overlap the minimization of ϕ_c would bring to non existing solutions, thus the best thing one can do is to take the solutions with lowest free energy and non negative complexity: thus for $q_{12} > q_{low}$ the dominating solutions are those corresponding to $\Sigma_c(f, q_{12}) = 0$.

The resulting curve of the free energy of the dominant solution, as a function of the overlap, is shown in figure 4-4. This curve is very similar to the one of V_3, with some small differences that will be later explained. In Chapter III we argued what could reasonably be the physical interpretation of the cuspid of V_3. Now one has a confirmation of that interpretation: q_{low} indeed corresponds to that value of the overlap at which the dominant states becomes finite ($\Sigma_c = 0$). Moreover we can also understand the meaning of the maximum, which turns out to be exactly at the same value in both the approaches: q_{max} is the overlap at which begins the anomalous reversing behaviour of the constrained complexity.

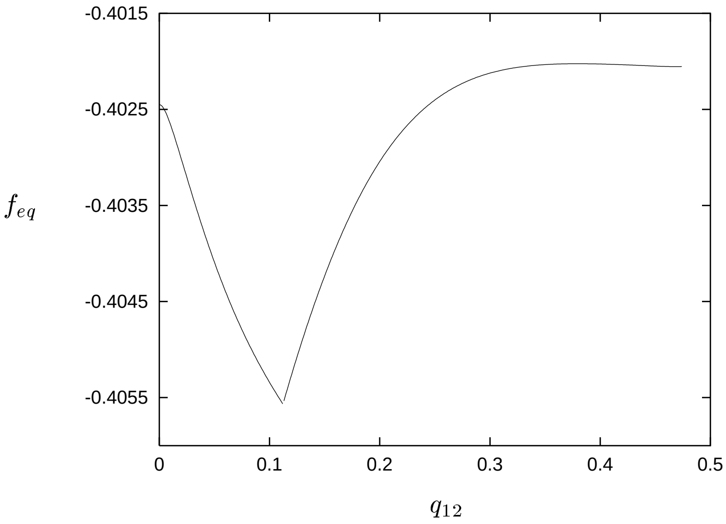

Figure 4-4: The energy density f_{eq} of the solutions dominating at distance q_{12} from the fixed equilibrium solution. The cuspid is at q_{low}=0.113 and the maximum is at q_{max}=0.360. The last point of the curve represents the distance of the nearest solutions.

4. An explanation of the differences between the two methods

Surely the curve shown in figure 4-4 is very similar to the one of $V_3(q_{12})$, however the two curves are not exactly the same. Why ? A reasonable explanation of this fact exists, but we have to go back again to replica 2 and analyze in a better way its process of thermalization.

Actually it is not exact to say that replica 2 catches the contribution of the states present at overlap q_{12} with the reference one. Indeed replica 2 is forced on the manifold defined by fixing q_{12} and in general the states of the system do not perfectly belong to this manifold, but only have a certain projection on it. Thus replica 2 catches the contribution of these projections and sees the true states only in this sort of deformed way. In the TAP language this can be expressed saying that replica 2 minimizes the TAP free energy f_{TAP} *in* the manifold fixed by q_{12}: the solutions found in this way are *not* the TAP solutions present at overlap q_{12}, which are obtained first minimizing f_{TAP} in its whole domain and then selecting the minima which have overlap q_{12} with the reference solution. These manifold-solutions instead consists for the most part in projections on the manifold of nearby true TAP solutions and their number is in general greater than the number of the TAP solutions at q_{12}.

In this context what actually happens is that, after thermalizing, replica 2 is fixed in one of the dominant manifold-solutions at overlap q_{12}, in the vicinity of a genuine TAP solution which has a slightly different overlap with the reference solution. Replica 3, on the other hand, perfectly thermalizes into this TAP solution giving the true values of its thermodynamical properties.

In its thermalization process replica 2 tries to optimize a generalized free energy function $\phi_2 = f_2 - T\Sigma_2(f_2, q_{12})$ relative to the manifold-solutions it finds at overlap q_{12} and not the function ϕ_c introduced in the previous section. The manifold complexity Σ_2 is different from Σ_c, since it is related to manifold-solutions and not to genuine ones. We can however realize that $\Sigma_2(f_2, q_{12})$ is related to the number of all those TAP solutions at overlaps $q \sim q_{12}$, whose projections on the manifold at overlap q_{12} all have the same reduced free energy f_2.

The minimization of ϕ_2 leads to a value $\bar{f}_2$ of the dominant manifold-solutions, but it still remains to understand what are the correspondent nearby TAP solutions which are in this way selected. How already said, there are TAP solutions at different distances which all have a projection of free energy $\bar{f}_2$ on the manifold. However these TAP solutions have in general different complexities and there will be a class with an exponentially higher number of solutions, which dominates among the others: this is the class of the TAP solutions selected by replica 2.

For example we can imagine that there are TAP solutions of a certain free energy f and manifold-projection $\bar{f}_2$ both at overlap $q_a > q_{12}$ and $q_b < q_{12}$. To understand what are among these the solutions selected by replica 2 we have to check which of them are entropically dominant. If we look at figure 4-2 4-3, we find that, given a certain value of f, the $\Sigma_c(f, q)$ decreases at increasing overlap if $q < q_{max}$ and behaves in the opposite way for $q > q_{max}$. This tells us that when $q_{12} < q_{max}$ the selected TAP solutions will be at overlap $q_b < q_{12}$ while when $q_{12} > q_{max}$ the selected TAP solutions will be at overlap $q_a > q_{12}$. A surprising confirmation of this mechanism is found within the results of the three-replica potential. Indeed, in correspondence of the minimum M_2 replica 3 equilibrates in the same TAP solution selected by replica 2, and therefore q_{13} in M_2 identifies the overlap of this solution with the reference state.

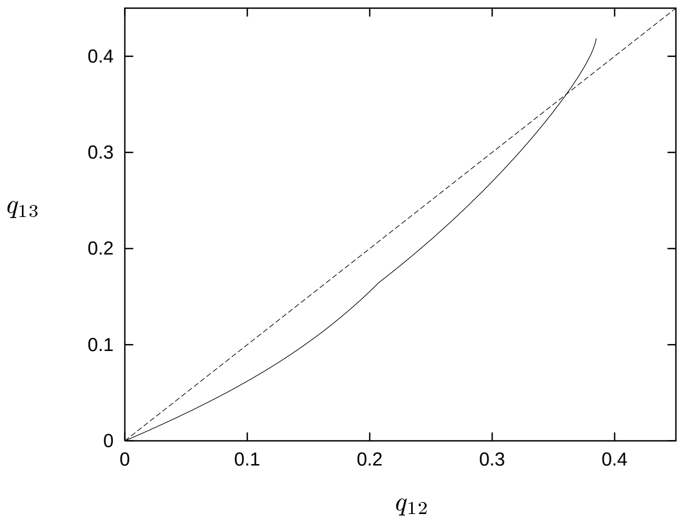

Figure 4-5: q_{13} in M_2 as a function of q_{12} at β=1.64; q_{EA}=0.546, $\bar{q}$=0.385.

If we look at the behaviour of q_{13} versus q_{12} in this minimum, we find the curve plotted in figure 4-5: we can see that when $q_{12} < q_{max}$ the value of q_{13}, is smaller than q_{12}; on the contrary when $q_{12} > q_{max}$ we have $q_{13} > q_{12}$. This is precisely what expected from the previous reasoning.

At this point we can also understand why the curve obtained from the constrained complexity is not exactly equal to the one given by the three-replica potential. Indeed we have seen that the two curves are related to a different mechanism of optimization. Given a certain overlap q_{12} with a reference equilibrium solution the first curve is determined by the minimization of the generalized free energy $\phi_c = f - T\Sigma_c(f, q_{12})$ and gives the free energy of the TAP solutions which dominate at that overlap. On the other hand, the second curve is determined by the minimization of the function $\phi_2 = f_2 - T\Sigma_2(f_2, q_{12})$ and gives the free energy of the TAP solutions whose projections on the manifold fixed by q_{12} identify the dominant manifold-solutions. However, it is evident that since manifold-solutions are projections of nearby genuine TAP solutions, the way in which the constrained thermalization on the manifold takes place is a direct consequence of how TAP solutions are actually distributed in the phase space, so that the two curves are qualitatively very similar.

One can see that the main differences are present in the first part of the curves, for $q_{12} < q_{low}$. Indeed at these values of the overlap the entropies Σ_c and Σ_2 are different from zero and greatly contributes in making different the two functions ϕ_c and ϕ_2. When $q_{12} = q_{low}$ the true TAP solutions dominant at q_{12} becomes finite, however the manifold-solutions at the same overlap correspond to TAP solutions at overlaps slightly smaller and are still exponentially numerous, therefore one has to high more q_{12} to observe an entropic collapse also in V_3. This is why $q_{low} < q_{rsb}$. We note that the value of the maximum is exactly at the same point $q_{12} = q_{max}$ for both the curves. This is due to the crucial role played by this value of the overlap in signaling a qualitative change of the distribution of the TAP solutions, which is directly manifested also by the manifold-solutions. Finally, the ending points of the two curves are different and it turns out that $q_{last} > \bar{q}$. This means that for $q_{12} > \bar{q}$ there are still TAP solutions, but the three-replica potential is not able to see them. The reason why this happens is still not clear. Surely one has to consider that the for $q_{12} > q_{max}$ the TAP solution in which replica 3 thermalizes is at overlap greater than q_{12} so that $\bar{q}$ can correspond to the case in which the selected TAP solution is actually at overlap q_{last}. However the value of $q_{13}(\bar{q})$, the true distance of the state of replica 3, remains definitely smaller than q_{last} suggesting that this explanation is not enough. Another possibility is that the last TAP solutions in the curve of figure 4-4 are not minima of f_{TAP}, but other kinds of saddle points, and therefore do not correspond to true states of the system. We will find a similar problem also in the completely different context of the barriers, discussed in the next chapter. However to better discuss this argument one has to develop a serious analysis of the nature of TAP solutions (see [43,28]), which can not be done here.

Chapter V: Barriers between metastable states

With the Real Replica method it is possible to give an estimate of the barriers between different metastable states. More precisely, one can evaluate the free energy density barriers which separate an equilibrium state from the metastable states present around it [24].

In the thermodynamic limit all the pure states are actually separated by infinite barriers and therefore have infinite life-times: if the system is in one of these states, it cannot escape and will remain there forever. However, this is not true if one considers N large, but finite. In this case the barriers are themselves very large, but finite, and diverge only when $N \to \infty$. One can then consider the energy and free energy density barriers $\Delta\mathcal{E}(N)/N$, $\Delta\mathcal{F}(N)/N$, and evaluate them in the thermodynamic limit to obtain well defined quantities:

$$\begin{aligned} \Delta E &= \lim_{N\to\infty} \frac{\Delta\mathcal{E}(N)}{N} \\ \Delta F &= \lim_{N\to\infty} \frac{\Delta\mathcal{F}(N)}{N} \; . \end{aligned} \tag{0.1}$$

Viceversa, if analytic computations of ΔE and ΔF are available, one can obtain reasonable estimates of the extensive barriers at finite N. The knowledge of these barriers turns out to be very important when analyzing the dynamics of a finite size system: if the system starts its evolution in an equilibrium state, after a certain time it will jump into a metastable state, this time being determined by the barrier the system has to cross. In this way a comparison between the static estimates of the barriers and the dynamical evaluation of the escape-times can enlighten about the actual behaviour of the system. For example, if the barrier separating two states is essentially an energetic barrier one expects the escape-time to scale exponentially with this barrier: $\tau_{esc} \sim \exp(\beta\Delta E(N))$. On the other hand, if this relation is violeted one expects an entropic factor to be relevant: when looking for a convenient way out from the starting state, the system has to try many times before finding the right one. This is what presumably happens in models which have very complicated landscapes and a great richness of metastable states, like the p-spin spherical model. In this case one has to refer to free-energy barriers and not to energetic ones.

The Real Replica method introduced in the previous chapters provides an interesting way to estimate statically the free energy density barriers, which in this model are the relevant ones. In this approach the system is forced to thermalize at certain imposed overlaps with some fixed configurations. In this way, varying the values of the overlaps, a sort of projection of the phase-space in the space of the overlaps is performed, each configuration of the system being mapped into its overlaps with the fixed configurations. The potential function evaluates the free energy cost payed to satisfy the constraints, and its minima in the overlaps-space correspond to pure states of the free system. In this context one can identify in the overlaps-space what is the most convenient path linking two different minima and evaluate the free energy cost payed along this path: this cost represents an estimate of the actual free energy density barrier between the states represented by the considered minima. Obviously the mapping that brings the phase space of the system into the space of the overlaps is not biunique, since there are many configurations which have the same distances with the fixed reference ones. In this way a path in the phase space is mapped into a single path in the overlaps-space, but the opposite is not true: there are paths in overlaps which do not correspond to any continuous path in terms of configurations. Due to this, the barriers evaluated in the overlaps-space through the potential function can only provide a lower bound for the free-energy density barriers actually separating two states, this estimate being more realistic when more refined potential functions are considered.

We will now show how this procedure works in the case of the potential functions previously introduced: the two-replica potential and the three-replica potential.

1. The estimate given by the two-replica potential

As discussed in Chapter II in this case there is only one fixed configuration, replica 1: each configuration of replica 2 is then mapped into its overlap q_{12} with replica 1. The potential function $V_2(q_{12})$ has two minima: a minimum in $q_{12}=0$ that corresponds to the equilibrium states orthogonal to replica 1, and the minimum M which corresponds to the same equilibrium state as replica 1. Since the overlap-space is unidimensional there is only one path linking these two minima which starts in M, passes for the maximum in $q_{12}=q_{max}$ and finally arrives in $q_{12}=0$. Since the highest point along this path is the maximum, the cost payed along it is

$$cost = V_2(q_{max}) - V_2(M) \ . \tag{1.1}$$

In this way one has a first rough estimate of the free energy density barrier to cross for going from an equilibrium state (M) to one of the equilibrium states far away from it ($q_{12}=0$), that is

$$\Delta F \geq V_2(q_{max}) - V_2(M) \ . \tag{1.2}$$

2. The estimate given by the three-replica potential

In this case there are two fixed reference configurations, replica 1 and replica 2, at mutual overlap q_{12}. The configuration τ of replica 3 is mapped into its overlaps (q_{13}, q_{23}) from the fixed ones. Thus, once fixed q_{12}, the overlaps-space is represented by the plane $\pi \equiv (q_{13}, q_{23})$ and the potential function $V_3(q_{12}|q_{13}, q_{23})$ is defined on it. V_3 has two non trivial minima: the minimum M_1 which corresponds to the equilibrium state of replica 1, and the minimum M_2 which corresponds to a metastable state at overlap q_{12} with replica 1. With varying q_{12} M_1 always corresponds to the same equilibrium state, while M_2 identifies with different metastable states, at different distances with replica 1. Fixed q_{12} one can look for the barrier separating the two states M_1 and M_2 via the analysis of the free energy contour given by V_3: one has to find in π the path linking M_1 to M_2 which minimizes the free energy cost. To this aim it is important the role of the saddles of the potential function in the overlaps-space. Indeed, as can be seen from the next figures, the problem of finding the best path from M_1 to M_2 reduces to single out the chain of saddles which minimizes the variation of V_3. The estimate of the barrier is then given by

$$\Delta F \geq V_(S_{max}) - V_3(M_1) \tag{2.1}$$

where S_{max} is the highest saddle crossed along the optimizing path to reach M_2.

It is possible to distinguish three different ranges:

i. $q_{12} < q^\star$: from Figure 5-1 we can see that in this range there are only two saddles, S_1 and S_2, and the path which links the two minima is then

$$M_1 \to S_1 \to S_2 \to M_2 \ . \tag{2.2}$$

Since the highest saddle is S_1, one has

$$\Delta F \geq \ V_3(S_1) - V_3(M_1) \ . \tag{2.3}$$

It is worth to note that the value of V_3 in M_1 and S_1 does not depend on q_{12} and therefore in this range the barrier is constant. Moreover one has

$$\begin{aligned} V_3(M_1) &= V_2(M) \\ V_3(S_1) &= V_2(q_{max}) \\ q_{13}(S_1) &= q_{max} \end{aligned} \tag{2.4}$$

therefore it is clear that S_1 plays the same role with respect to M_1 as the role played by q_{max} with respect to M so that the estimate (2.3) coincides with the one given by the two-replica potential. The most natural hypothesis is that the barrier which separates an equilibrium state (M or M_1) from metastable states very far from it (small values of q_{12} in three-replica potential), is the same as the barrier separating it from the other orthogonal equilibrium states ($q_{12} = 0$ in the two-replica potential).

ii. $q^\star < q_{12} < q'$: at $q^\star$ S_2 becomes higher than S_1 (see Figure 5-2) and so in this range the optimizing path is the same as in (2.2), but the barrier is

$$\Delta F \geq \ V_3(S_2; q_{12}) - V_3(M_1) \tag{2.5}$$

that depends on q_{12}. We note from Figure 5-2 that in this range there is a value of q_{12} at which a new saddle S appears together with a maximum; however, since for $q_{12} < q'$ we have $V_3(S) > V_3(S_2)$, the path that minimizes the variation of V_3 still is (2.2).

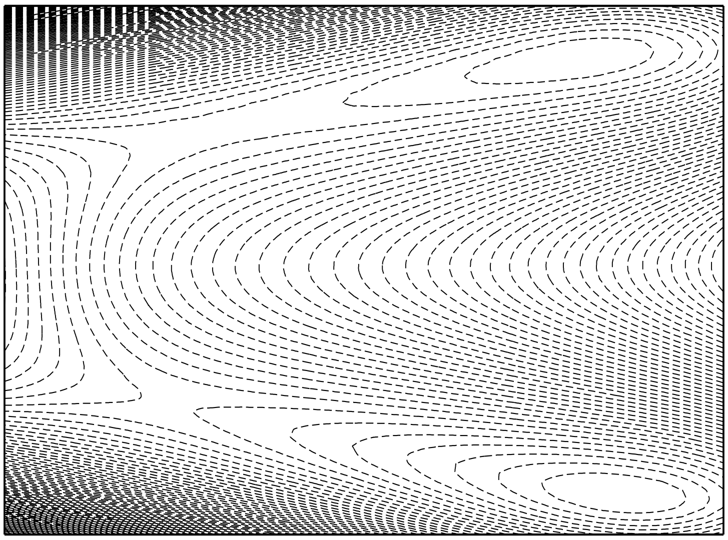

Figure 1: The contour lines of V_3 for q_{12}=0.25 and β=1.64. The axis are $x=\frac{1}{\sqrt{2}}(q_{13}+q_{23})$ in the range [0.25:0.6], and $y=\frac{1}{\sqrt{2}}(q_{13}-q_{23})$ in the range [−0.3,0.3]. The two minima are visible on the right: M_1 (up) and M_2 (down); on the left the two saddles: S_1 (up) and S_2 (down).

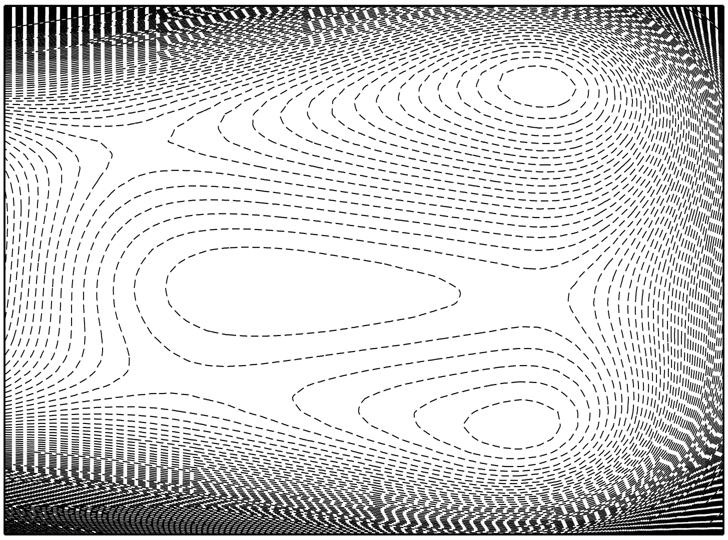

Figure 2: The contour lines of V_3 for q_{12}=0.36. The axis are the same as in Figure 1, with ranges $x\in$[0.35,0.75] and $y\in$[−0.2,0.2]. The new saddle S is clearly visible on the right, in the middle between the two minima.

iii. $q' < q_{12} < \bar{q}$: at q' the path that minimizes the variation of V_3 suddenly changes because S becomes lower than S_2; so we have

$$M_1 \to S \to M_2 \tag{2.6}$$

and

$$\Delta F \geq\ V_3(S;q_{12}) - V_3(M_1)\ . \tag{2.7}$$

This situation holds up to $q_{12} = \bar{q}$, when M_2 disappears merging with S.

The whole behaviour of V_3 in the three saddles is shown in Figure 5-3. If we then consider for the different ranges of q_{12} the relevant saddle, we obtain the estimate of the barrier as a function of q_{12}: Figure 5-4 shows the resulting behaviour.

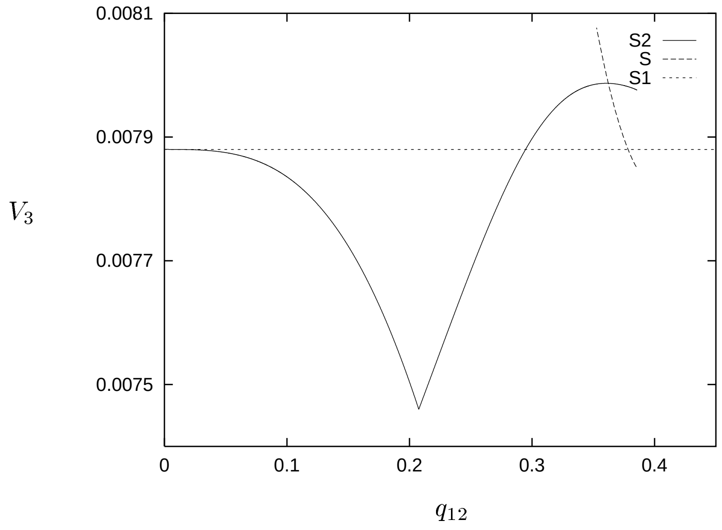

Figure 4-3: V_3 evaluated in the three saddles S_1, S_2 and S as a function of q_{12}. For β=1.64, q^*=0.295 and q'=0.362.

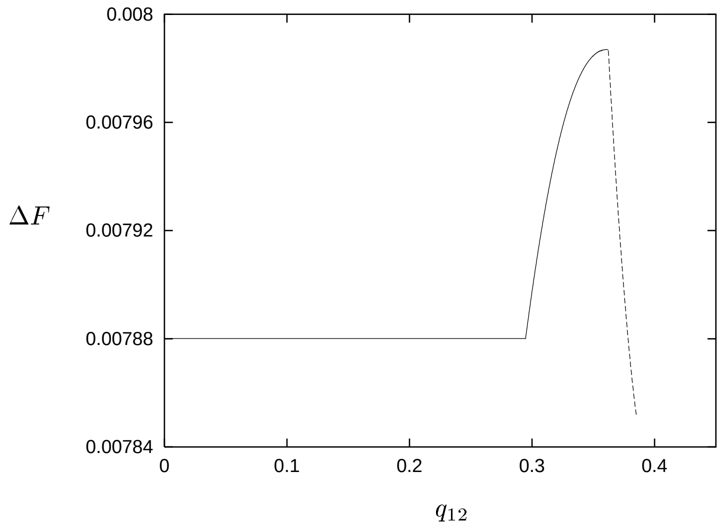

Figure 4-4: The free energy barrier ΔF as a function of q_{12}.

3. The physical meaning of the saddles

We have seen that the saddles of the three-replica potential have an important role in the determination of the barriers. It can then be interesting to analyze in more details the properties of these saddles. As we shall see this will enable us to give a possible interpretation of the barriers in terms of TAP solutions.

- The maximum of the two-replica potential determines the barrier between the equilibrium state of replica 1, and the equilibrium states orthogonal to it. We can try to understand more on this maximum looking at the sub-matrix Q_{22} in $q_{12} = q_{max}$. It turns out that Q_{22} is broken and, more than this, the parameter r_1 of this matrix and the value of $V_2(q_{max})$ satisfy TAP equations. Following the usual interpretation for the RSB solution we can then argue that in this point replica 2 has access to a finite number of TAP solutions of individual free energy density $f_{TAP} = V_2(q_{max})$. In the previous chapter we have studied the overlap distribution of the TAP solutions around a reference equilibrium solution. In particular we have also obtained the spectrum of the dominant solutions at the various overlaps with the reference one: it turns out that the dominant solutions with greatest free energy density are found *precisely* at overlap q_{max}, as can be clearly seen from figure 4-5, and have the free energy density f_{TAP} just found for the maximum of V_2. Therefore we can hypothesize the following explanation: The best escape-way the system can choose to go from an equilibrium state to another orthogonal equilibrium state provides for passing via other states which lie in between. In this context the barrier is determined by those among these states which have the highest free energy, i.e. by the states which are at overlap q_{max} with the starting equilibrium state.

- The saddle S_1 of the three-replica potential determines the barrier between the equilibrium state of replica 1 and a metastable state at low overlap q_{12} with it. We have seen that this saddle is analogous to the maximum of the two-replica potential, and indeed also in this case the sub-matrix Q_{33} is RSB, with s_1 and V_3 satisfying the TAP equations. Thus replica 3 has access to a finite number of TAP solutions with free energy density $f_{TAP} = V_3(S_1) = V_2(q_{max})$ which are at overlap $q_{13} = q_{max}$ with replica 1. Therefore the best-escape way for the system still provides for passing via some states which lie between the starting state and the final one, and the barrier has the same interpretation as in the previous case.

- The saddle S_2 begins to determine the barrier for $q_{12} = q^\star$, however it is present in the plane π for each value of $q_{12} \leq \bar{q}$. If we analyze the overlap matrix Q_{33} we find that S_2 has qualitatively the same features as S_1: Q_{33} is indeed broken and s_1 and $V_3(S_2)$ still satisfy the TAP equations. Thus also in this case replica 3 has access to a finite number of TAP solutions, now with free energy density $f_{TAP} = V_3(S_2)$. However in this case $V_3(S_2)$ is not constant with varying q_{12}, this meaning that S_2 identifies different kinds of TAP solutions when different values of q_{12} are chosen. Moreover, if we look at the value of q_{13} and q_{23} we discover that this saddle is much nearer to the metastable state corresponding to M_2 than to the reference equilibrium state M_1 (see figures 5-1 and 5-2). This suggests that S_2 may have a meaning analogous to S_1 but this time with respect to the metastable state M_2: it identifies the dominant TAP solutions around M_2 which have the highest free energy density. Indeed, for $q_{12} = q^\star$ when both M_1 and M_2 correspond to equilibrium states, the two saddles have exactly the same properties. To check better this point we can refer once again to the constrained complexity of the previous chapter: we choose as reference TAP solution the TAP solution corresponding to the metastable state M_2, and analyze the overlap distribution of the other TAP solutions around it. If we look at the resulting spectrum of the dominant solutions, we find that the dominant solutions with highest free energy are exactly at overlap $q = q_{23}(S_2)$ with the reference solution, and have free energy density $f_{TAP} = V_3(S_2)$. This strongly supports our hypothesis.

We can now outline what is the role of the two saddles S_1 and S_2 in determining the barrier. We have considered two different states: one of them (M_1) is an equilibrium state while the other (M_2) is in not in general of equilibrium and is at overlap $\sim q_{12}$ with the first one. Each one of these two states is surrounded by many other states, which can be found with continuity at various distances from them. When N is large but finite if the system starts in M_1 it will have to pass via some of these states to reach M_2. The system tries to follow the best way, and this reasonably implies that it passes for those states which, in a given point along the path, minimize the free energy cost. From the complexity approach we know that, given a state, the dominant states around it are disposed in such a way to form a free energy maximum at small distance from it. We can then argue that the system will encounter two different free energy barriers: the first one, identified by the saddle S_1, when leaving the starting state, and the second one, identified by the saddle S_2, when approaching the final state. The global free energy density barrier will then be given in the thermodynamic limit by the greatest between these two barriers. For values of q_{12} lower than $q^\star$ the metastable state identified by M_2 has free energy density lower than the equilibrium one, as can be seen from figure 3-1. In this case we find with the complexity approach that the dominant states around it forms a free energy maximum which is lower than the one formed around an equilibrium state. Therefore the saddle S_1 is the highest one and determines the barrier. The opposite holds when q_{12} is greater than $q^\star$, even if at a certain point we must be careful and include in the discussion also the new saddle S.

- The saddle S is present only when high enough values of q_{12} are considered. If we look at Q_{33} we discover that in this saddle this overlap matrix is surprisingly symmetric. Moreover s_1 and $V_3(S)$ satisfy the TAP equations. Following the adopted interpretation of an RS solution, we are lead to say that replica 3 thermalizes in correspondence of a single TAP solution. However this TAP solution is *not* in correspondence of a true state of the system otherwise the potential would form a minimum and not a saddle. A reasonable explanation is that S actually corresponds to a TAP solution, but this solution is a saddle and not a minimum of the TAP free-energy f_{TAP}. In the TAP approach only the minima of f_{TAP} correspond to pure states of the system, however it turns out [28] that the minima are entropically dominant over the saddles so that it is really rare to find a TAP solution which is a saddle. This is the reason why one does not in general discuss this point. However when high values of the imposed overlaps are considered replica 3 is forced in very small regions of the phase space and the entropic factors are not important anymore: if a TAP saddle is present in that region it can thus be revealed. If we accept the idea that S is a TAP saddle it still remains to give it a sensible physical interpretation. To this aim one can look at the values of $q_{13}(S)$ and $q_{23}(S)$ to discover that they are both very high. This fact means that S is very close to M_1 and M_2 and suggests that S represents a *real* saddle in the phace space, the saddle which links the two states corresponding to M_1 and M_2.

We can now complete our scenario on the barriers. When q_{12} is enough high the states M_1 and M_2 are sufficiently near to have a path in the phase space which directly connects them without passing via other states. The barrier along this path is given by the saddle S. However for $q_{12} < q'$ the best way the system can choose is still the ones which passes for other states and the barrier continues to be determined by S_2. On the other hand for $q_{12} \geq q'$ the direct way becomes the optimizing one and the barrier is determined by S. We conclude noting that if the conjecture on the nature of this saddle is true and S actually corresponds to a real saddle in the phase space, then expression (2.7) would give the *exact* free energy density barrier and not only a lower bound.

4. Conclusions

In this chapter we have obtained a statical estimate of the free energy density barriers separating an equilibrium state from other metastable states at various distances from it. The knowledge of these barriers enable us to outline a possible dynamical scenario when the size N of the system is large but finite.

If the system starts its evolution in an equilibrium state, after a certain large but finite time it will jump into a metastable state close to it. From figure 5-4 we can see that the smallest free energy barrier is the one which separates the equilibrium state from the metastable state nearest to it, which is at overlap $\bar{q}$: the system will then reasonably jump into this state. The successive evolution is determined by the disposition of the states and the barriers around this new state and we actually do not know it. However we note that the free energy density barrier separating the metastable state at $\bar{q}$ from the starting equilibrium state is given by

$$\Delta F = V_3(S) - V_3(M_2) \mid_{\bar{q}} \quad . \tag{4.1}$$

When $q_{12} = \bar{q}$ the saddle S and the minimum M_2 merge together and therefore this barrier is vanishing. We can then argue that the most convenient thing the system can do is to jump back into the original equilibrium state. This reasoning is not strictly valid if the first jump brings the system in a metastable state which is not precisely the nearest one. The free energy density barrier to return back is not in this case vanishing, but remains small if the metastable state is sufficiently close and we can imagine that the back way still remains the most probable. If this is true the system continues to jump from the starting equilibrium state into a near metastable state and then back into the same equilibrium state. This behaviour will take place until when, after many attempts, the system finds the less probable way towards more distant states and the correlation with the initial state is finally lost.

If we look at the overlap $q(t) = C(t, 0)$ between the configuration at time zero and the configuration at time t we then expect a form typical of a punctuated equilibrium: exponentially long periods of stasis where $q(t)$ fluctuates around a value which corresponds to a local equilibrium state punctuated with fast variations of $q(t)$ which corresponds to jumps between one local equilibrium and other local equilibrium states. Some numerical simulations done with this model seem to confirm this scenario, even if, for computational reasons, only small sizes can be considered and a quantitative comparison with the analytical results is therefore at present difficult.

Conclusions

In this thesis we have discussed how to investigate the structure of the states in mean field spin glass models. This problem becomes particularly interesting when considering models with discontinuous statical transition. In this case the phase space of the system is broken into a huge number of ergodic components which are relevant in determining both the statical and dynamical behaviour. The equilibrium of the system is actually a collective effect and is given by a class of exponentially numerous pure states, which have individually a vanishing weight, but result dominant grace to their entropic contribution. In this context the equilibrium states are not the stable ones, but identifies at each different temperature with a different class of metastable states. Metastable states therefore cannot be disregarded and their structure in the phase space becomes a primary question. The usual statical approaches are not able to provide enough information on this topic, the structure of the states remains in this sense hidden and non standard methods must be introduced to reveal it.

In the context of the Real Replica approach we have developed and discussed the effective Potential method for the p-spin spherical model. With the three-replica potential we have been able to show that this model has a highly non trivial structure of the states in the phace-space, which exhibits correlations both in distance and in energy. We have reconstruct the local environment of a given equilibrium state of the system revealing the disposition of the metastable states around it and giving some estimates of the free energy density barriers separating different metastable states. This kind of information enables to hypothesize the dynamical behaviour of the system when N is large but finite and is an important step towards the comprehension of analogous short range models.

We have compared the results obtained with the three-replica potential with the ones given by the constrained complexity, finding that the two methods are perfectly consistent and mutually confirm. We have understood and explained the frame outlined with the potential method in terms of TAP solutions, giving sensible interpretation both of the minima and of the saddles of the potential function.

We have performed our analysis for the p-spin spherical model, but we are reasonably convinced that the same procedure can be successfully adopted also for other models which present the same features: the presence of many metastable states relevant in determining the behaviour of the system, whose structure and properties can not be revealed with standard strategies. Besides the other spin glass models of the second class, interesting cases are surely constituted by structural glasses, super-conducting Josephson arrays and models of biological systems.

We would like to comment at this point an important difference between the potential and the complexity method. Surely the constrained complexity gives a wider information providing a complete entropic distribution of the states in the phase space while, as we have seen, the three-replica potential catches only the contribution of some of these states. However to define and compute the constrained complexity one needs as a starting point a set of mean field equations for the local magnetizations. For the p-spin spherical model these equations are easily obtained with the cavity method, but the same cannot be true also for more complicated models. On the other hand the potential function can in principle be computed for each sort of model and is in this sense more general.

References

[1] Sherrington D and Kirkpatrick S 1975 *Phys. Rev. Lett.* **35** 1792

[2] Mézard M, Parisi G and Virasoro M A 1986 *Spin Glass Theory And Beyond*, World Scientific Publishing, Singapore

[3] Cugliandolo L F and Kurchan J 1994 *J. Phys. A: Math. Gen.* **27** 5749

[4] Bouchaud J P, Cugliandolo L F, Kurchan J, Mézard M in *Spin-glasses and random fields*, A. P. Young Ed. (World Scientific)

[5] Crisanti A and Sommers H-J 1992 *Z. Phys.* B **87** 341

[6] Gross D J and Mézard M 1984 *Nucl. Phys. B* **240** 431

[7] Kirkpatrick T R and Thirumalai D 1987 *Phys. Rev.* B **36** 5388. Kirkpatrick T R and Thirumalai D 1988 *Phys. Rev.* B **37** 4439. Thirumalai D and Kirkpatrick T R 1988 *Phys. Rev.* B **38** 4881. Kirkpatrick T R and Thirumalai D 1989 *J. Phys. A: Math. gen.* **22** L149.

[8] de Santis E Parisi G Ritort F cond-mat 9410093

[9] Cugliandolo L F and Kurchan J 1993 *Phys. Rev. Lett.* **71** 173

[10] Crisanti A, Horner H and Sommers H-J 1993 *Z. Phys.* B **92** 257

[11] Kirkpatrick T R and Wolynes P G 1987 *Phys. Rev.* A **35** 3072. Kirkpatrick T R and Wolynes P G 1987 *Phys. Rev.* B **36** 8552

[12] Horner H 1984 *Z. Phys.* B **57** 29

[13] Götze W in *Liquids, freezing and the glass transition* eds. Hansen J P Levesque D and Zinn-Justin J Editors, Les Houches 1989.

[14] Kirkpatrick T R Thirumalai D and Wolynes P G 1987 *Phys. Rev.* **36** 8552

[15] Parisi G *Slow dynamics in glasses* cond-mat 941115, cond-mat 9412034

[16] Bouchaud J P Cugliandolo L F Kurchan J and Mézard M 1996 *Physica A* **226** 243

[17] Parisi G 1979 *Phys. Rev. Lett.* **23** 1754

[18] Parisi G 1980 *J. Phys. A: Math. Gen.* **13** L115

[19] Parisi G 1980 *J. Phys. A: Math. Gen.* **13** 1887

[20] Mézard M, Parisi G, Sourlas N, Toulouse G and Virasoro M A 1984 *J. Physique* **45** 843

[21] Kurchan J, Parisi G and Virasoro M A 1993 *J. Phys. I France* **3** 1819

[22] Franz S and Parisi G 1995 *J. Phys. I France* **5** 1401

[23] Cavagna A, Giardina I and Parisi G 1997 *J. Phys. A: Math. Gen* **30** 4449

[24] Cavagna A, Giardina I and Parisi G 1997 cond-mat 9702069

[25] Thouless D J, Anderson P W and Palmer R G 1977 *Philos. Mag.* **35** 593

[26] Crisanti A and Sommers H-J 1995 *J. Phys. I France* **5** 805

[27] Cavagna A, Giardina I and Parisi G 1997 *J. Phys. A: Math. Gen* **30** 7021

[28] Cavagna A, Giardina I and Parisi G 1997 cond-mat 9710272

[29] Gardner E *Nucl. Phys. B* **257** 747

[30] Barrat A 1997, thèse de doctorat de l'université Paris VI, cond-mat 9701031

[31] De Dominicis C and Young A P 1983 *J. Phys. A: Math. Gen.* **29** L81

[32] Nieuwenhuizen Th M 1996 *Phys. Rev. Lett.* **74** 4289

[33] Bouchaud J P 1992 *J. Phys. I France* **2** 1705

[34] Bouchaud J P and Dean D S 1995 *J. Phys. I France* **5** 265

[35] Kurchan J and Laloux L 1996 *J. Phys. A: Math. Gen* **29** 1929

[36] Franz S, Parisi G and Virasoro M A 1992 *J. Phys. I France* **2** 1869

[37] Franz S and Parisi G 1997 *Phys. Rev. Lett.* **79** 2486

[38] Franz S and Parisi G 1997 *Effective potential in glassy systems: theory and simulations* cond-mat 9711215

[39] Monasson R 1995 *Phys. Rev. Lett.* **75** 2847

[40] Franz S 1996, private communication

[41] Barrat A, Burioni R and Mézard M 1996 *J. Phys. A: Math. Gen* **29** L81

[42] Barrat A and Franz S cond-mat 9708154

[43] Kurchan J 1991 *J. Phys. A: Math. Gen* **24** 4969